



Leveraging 35 years of forest research in the southeastern U.S. to constrain carbon cycle predictions: regional data assimilation using ecosystem experiments

R. Quinn Thomas^{1*}, Evan Brooks¹, Annika Jersild¹, Eric Ward², Randolph Wynne¹, Timothy J. Albaugh¹, Heather Dinon Aldridge³, Harold E. Burkhart¹, Jean-Christophe Domec^{4,5}, Thomas R. Fox¹, Carlos A. Gonzalez-Benecke⁶, Timothy A. Martin⁷, Asko Noormets⁸, David A. Sampson⁹, Robert O. Teskey¹⁰

¹Department of Forest Resources and Environmental Conservation, Virginia Tech, USA,

²Climate Change Science Institute and Environmental Sciences Division, Oak Ridge National Laboratory, USA,

³State Climate Office of North Carolina, North Carolina State University, USA,

⁴Bordeaux Sciences Agro, UMR 1391 INRA-ISPA, 33175 Gradignan Cedex, France,

⁵Nicholas School of the Environment, Box 90328, Duke University, Durham, NC 27708, USA,

⁶Department of Forest Engineering, Resources and Management, Oregon State University, USA,

⁷School of Forest Resources and Conservation, University of Florida, USA,

⁸Department of Forestry and Environmental Resources, North Carolina State University, USA,

⁹Decision Center for a Desert City, Arizona State University, USA,

¹⁰Warnell School of Forestry and Natural Resources, University of Georgia, USA,

*Corresponding author: R. Quinn Thomas (rqthomas@vt.edu)



24 **Abstract**

25
26 Predicting how forest carbon cycling will change in response to climate change and management
27 depends on the collective knowledge from measurements across environmental gradients,
28 ecosystem manipulations of global change factors, and mathematical models. Formally
29 integrating these sources of knowledge through data assimilation, or model-data fusion, allows
30 the use of past observations to constrain model parameters and estimate prediction uncertainty.
31 However, the influence of different experimental treatments on those predictions depends on the
32 exact methods and techniques used for data assimilation. Here, we introduce a hierarchical
33 Bayesian DA approach (Data Assimilation of Pine Plantation Ecosystem Research, DAPPER)
34 that uses observations of carbon stocks, carbon fluxes, water fluxes, and vegetation dynamics
35 from loblolly pine plantation ecosystems across the Southeastern U.S. to constrain parameters in
36 a modified version of the 3-PG forest growth model. The observations included major
37 experiments that manipulated atmospheric carbon dioxide (CO₂) concentration, water, and
38 nutrients, along with non-experimental studies that spanned environmental gradients across an
39 $8.6 \times 10^5 \text{ km}^2$ region. We optimized regionally representative posterior distributions for the most
40 sensitive model parameters, which dependably predicted data from plots withheld from the data
41 assimilation. The posterior distributions of parameters associated with ecosystem responses to
42 CO₂, precipitation, and nutrient addition, along with the corresponding regional changes in
43 production associated with nutrient fertilization and drought, depended on how the experimental
44 data were assimilated. In particular, assimilating nutrient addition experiments reduced the
45 predicted sensitivity to nutrient fertilization while assimilated water manipulation experiments
46 increased the sensitivity to drought. Further, it was necessary to assimilate data from the CO₂
47 experimental enrichment site before other studies to constrain the parameters associated with the



48 influence of CO₂ on canopy photosynthesis. The ambient CO₂ plots were numerous and had a
49 large contribution to the cost function compared to the low number of elevated CO₂ plots (289
50 ambient vs. 5 elevated plots). Overall, we demonstrated how three decades of research in
51 southeastern U.S. planted pine forests can be used to develop data assimilation techniques that
52 use multiple locations, multiple data streams, and multiple ecosystem experiment types to
53 optimize parameters. This approach allows for future predictions to be consistent with a rich
54 history of ecosystem research across a region.

55

56



57 **1 Introduction**

58 Forest ecosystems absorb and store a large fraction of anthropogenic carbon dioxide (CO₂)
59 emissions (Le Quere et al., 2015; Pan et al., 2011) and supply wood products to a growing
60 human population (Shvidenko et al., 2005). Therefore, predicting future carbon sequestration and
61 timber supply is critical for adapting forest management practices to future environmental
62 conditions and for using forests to assist with reduction of atmospheric CO₂ concentrations. The
63 key sources of information for developing these predictions are results from global change
64 ecosystem manipulation experiments, observations of forest dynamics across environmental
65 gradients, and process-based ecosystem models. The challenge is integrating these three tools
66 into a common framework for creating probabilistic predictions, or forecasts (based on (Luo et
67 al., 2011a)), that provide information on both the expected future state of the forest and the
68 probability distribution of those future states.

69
70 Data assimilation (DA), or data-model fusion, is an increasingly used framework for integrating
71 ecosystem observations into ecosystem models (Luo et al., 2011a; Niu et al., 2014; Williams et
72 al., 2005). DA integrates observations with ecosystem models through statistical, often Bayesian,
73 methods that generate probability distributions for ecosystem model parameters and initial states.
74 DA allows for the explicit accounting of observational uncertainty (Keenan et al., 2011), the
75 incorporation of multiple types of observations with different time scales of collection
76 (Richardson et al., 2010), and the representation of prior knowledge through informed parameter
77 prior distributions or specific relationships among parameters (Bloom and Williams, 2015).
78 Using DA to parameterize ecosystem models with observations from multiple locations that
79 leverage environmental gradients and from ecosystem manipulation experiments will allow for



80 forecasts to be consistent with the rich history of global change research in forest ecosystems.
81
82 Ecosystem manipulation experiments provide a controlled environment in which data collected
83 can be used to describe how forests acclimate and operate under altered environmental
84 conditions (Medlyn et al., 2015). These data may be used to constrain model parameters that are
85 associated with specific physiological functions associated with, for example, carbon allocation
86 and turnover as related to the controlled manipulation. Furthermore, the assimilation of
87 experiments may increase parameter identifiability (reducing equifinality (Luo et al., 2009)),
88 where two parameters have compensating controls on the same processes, by isolating the
89 response to a manipulated driver. For example, carbon assimilation and primary productivity can
90 be modeled as a light and temperature controlled process that is adjusted by nutrients, water, and
91 atmospheric CO₂ concentration. In this case, the productivity may mathematically be equal
92 between a parameterization that has high potential conversion of light to photosynthesis (high
93 quantum yield) but low relative nutrient availability and a parameterization with low quantum
94 yield but high relative nutrient availability. Therefore, the challenge is that the same rate of
95 production can emerge from different contributions of environmental controls.
96
97 For future predictions with changing environmental conditions, the relative contribution of each
98 environmental control should be separated in order to correctly parameterize the sensitivity to
99 changes in the environment. Key examples of existing and past ecosystem experiments that have
100 the potential to isolate specific parameters in DA include CO₂ enrichment, water manipulation,
101 nutrient addition, and elevated soil temperature experiments. Many of these experiments are
102 common, particularly when including nutrient addition experiments in managed forests. Other



103 types of experiments are less common, but the few sites with the experiments, such as whole-
104 ecosystem CO₂ enrichment, include intensive measurements of numerous carbon pools and
105 fluxes required for model optimization.
106
107
108 Developing optimized parameters that apply to a region requires assimilating observations that
109 span environmental gradients to support the application of model predictions to a range of
110 climatic conditions, nutrient availabilities, and soil water dynamics. Therefore, the DA of
111 multiple research sites across a region is an important extension of prior DA research focused on
112 DA at a single site with multiple types of observations (Keenan et al., 2012; Richardson et al.,
113 2010; Weng and Luo, 2011). Incorporating multiple locations that include global change
114 experiments in DA is associated with numerous challenges. First, prior research has
115 demonstrated that high frequency observations (i.e., daily, or more frequent, net ecosystem
116 exchange observations) can overwhelm the contribution of low frequency observations (i.e.,
117 annual tree diameter measurements) to the cost-function used for optimization (Richardson et al.,
118 2010), resulting in a parameter set that predominately represents the high-frequency dynamics.
119 DA of ecosystem experiments and regional observations can present similar issues because key
120 contrasts isolated in an ecosystem experiment with relatively few plots may be overwhelmed by
121 the contribution of more numerous regional observations from non-manipulated plots. For
122 example, whole ecosystem CO₂ enrichment experiments are uncommon but are the only
123 observations representing ecosystem dynamics in an environment with over 550 ppm
124 atmospheric CO₂ (McCarthy et al., 2010). Therefore, DA techniques may be required that assign
125 additional weight to unique, but rare, experiments in the DA approach. As an example, a multi-



126 stage Bayesian approach could be used where the observations from the unique experiment are
127 assimilated first and the posteriors from that assimilation are used as priors for the assimilation
128 of the remaining observations. Second, DA requires using highly simplified ecosystem models
129 because many DA methods use millions of iterations to explore parameter distributions and these
130 iterations have to be applied to both control and manipulated treatments. However, in tension
131 with the need for simple models in DA, more complex models that simulate carbon, water, and
132 nutrient dynamics are also needed to fully leverage the diversity of ecosystem manipulation
133 experiments. Monthly time-scale models of ecosystem processes may be well suited to overcome
134 these challenges for application to predicting changes in biomass over decades in response to
135 global change. First, the contribution of monthly flux and annual biomass measurements to the
136 optimized cost function is more similar in monthly than daily models (12:1 vs. 365:1). Second,
137 they are computationally more efficient than daily models commonly used in DA, allowing data
138 spanning hundreds of plots and multiple decades to be assimilated. Finally, DA is able to
139 calibrate parameters associated with carbon, nitrogen, and water cycles so that they are
140 appropriate for an aggregated monthly time step, helping prevent potential issues associated
141 when applying daily parameterizations to coarser temporal time-steps.

142

143 Southeastern U.S. planted pine forests are ideal ecosystems for exploring the application of DA
144 to carbon cycle and forest production predictions. These ecosystems are dominated by loblolly
145 pine (*Pinus taeda* L.), thus allowing for a single parameter set to be applicable to a large region
146 containing many soil types and climatic gradients. Loblolly pine represents more than one half of
147 the standing pine volume in the southern United States (11.7 million ha) and is by far the single
148 most commercially important forest tree species for the region, with more than 1 billion



149 seedlings planted annually (Fox et al., 2007; McKeand et al., 2003). There is also a rich history
 150 of experimental research focused on global change factors including region-wide nutrient
 151 addition (Albaugh et al., 2016; Carlson et al., 2014; Raymond et al., 2016), water exclusion
 152 (Bartkowiak et al., 2015; Tang et al., 2004; Ward et al., 2015; Will et al., 2015), and water
 153 addition experiments (Albaugh et al., 2004; Allen et al., 2005; Samuelson et al., 2008). The
 154 region also includes a long-term ecosystem CO₂ enrichment study (McCarthy et al., 2010).
 155 Furthermore, many of these experiments are multi-factor with water exclusion-by-nutrients (Will
 156 et al., 2015), water addition-by-nutrients (Albaugh et al., 2004; Allen et al., 2005; Samuelson et
 157 al., 2008), and CO₂-by-nutrients treatments (McCarthy et al., 2010; Oren et al., 2001). Beyond
 158 experimental treatments, Southeastern U.S. loblolly pine ecosystems include at least two eddy-
 159 covariance sites with high frequency measurements of carbon and water fluxes along with
 160 biometric observations over many years (Noormets et al., 2010; Novick et al., 2015), and sites
 161 with multi-year sap flow data (Ewers et al., 2001; Gonzalez-Benecke and Martin, 2010; Phillips
 162 and Oren, 2001). Finally, there are available studies that include plots that span the regional
 163 environmental gradients and extend back to the 1980s (Burkhart et al., 1985). Overall, the high
 164 availability of observations of biomass stocks, leaf area index (LAI), carbon fluxes, water fluxes,
 165 and vegetation dynamics that span the past 35 years in loblolly pine ecosystems, including plots
 166 with experimental manipulation and plots across environmental gradients, is well suited to
 167 potentially constrain model parameters and predictions of how carbon cycling responds to
 168 environmental change.

169

170 Our objective was to develop a DA approach that integrated diverse data from multiple locations,
 171 including ecosystem experiments, for predicting how forest productivity may respond to global



change. We applied DA techniques to optimize a monthly-time step, simple forest productivity model using southeastern U.S.-wide experimental (nutrient addition, CO₂ enrichment, and water manipulations) and non-experimental data from 35 years of loblolly pine plantation research in the region. Our DA approach, DAPPER (Data Assimilation of Pine Plantation Ecosystem Research), is unique in its focus on simultaneously assimilating observations from multiple locations, experimental types, and data streams into a simple ecosystem model that includes carbon, water, and (implicitly) nutrients using a hierarchical Bayesian technique to develop parameter distributions. We used the DAPPER system to evaluate the sensitivity of biomass predictions and parameter distributions to the inclusion of ecosystem experiments in DA and to predict the regional sensitivity of forest production to nutrient fertilization and drought.

182

183 **2 Methods**

184

185 **2.1 Ecosystem Model**

We used a modified version of the Physiological Principles Predicting Growth (3-PG) Model to simulate vegetation dynamics in loblolly pine stands (Bryars et al., 2013; Gonzalez-Benecke et al., 2016; Landsberg and Waring, 1997). 3-PG is a stand-level vegetation model that runs at the monthly time-step and includes vegetation carbon dynamics and a simple soil water bucket model (Figure 1). While a complete description of the 3-PG model and our modifications can be found in the Supplemental Material, the key concept for interpreting the results is that gross primary productivity (GPP) was simulated using a light-use efficiency approach where the absorbed photosynthetically active radiation (APAR) was converted to carbon based on a quantum yield. Quantum yield was simulated using a parameterized maximum quantum yield



(α) that was modified by environmental conditions including air temperature, atmospheric CO₂, available soil water and soil fertility. The available soil water and soil fertility modifiers were values between 0 and 1, while the atmospheric CO₂ modifier had a value of 1 at 350 ppm and values greater than 1 at higher CO₂ concentrations.

Elevated CO₂ modified tree physiology by increasing quantum yield, based on an increasing but saturating relationship with atmospheric CO₂. We also added a function where the allocation to foliage relative to stem biomass decreased as atmospheric CO₂ increased. Available soil water and quantum yield were positively related through a logistic relationship between relative available soil water and the quantum yield modifier, where relative available soil water was the ratio of simulated available soil water to a plot-level maximum available soil water. Soil fertility and quantum yield were proportionally related, where quantum yield was scaled by an estimate of relative stand-level fertility where a value of 1 was the maximum fertility. The fertility modifier (FR) was constant throughout a simulation of a plot and was either based on site characteristics or directly optimized as a stand-level parameter. Here we used site-index, a measure of the height of a stand at a specified age (25 years), and the 35-year mean annual temperature as site characteristics to predict FR. For a given climate, site index captures differences in soil fertility, where a lower site index corresponded to a site with lower fertility. However, regional variation in site index also included the influence of climate on growth rates that were already accounted for in the other environmental modifiers in the 3-PG model. To account for the climatic influence on site index, a long-term climate variable (35-year mean annual temperature) was included in the empirical relationship that predicted FR as an increasing, but saturating, function of site index. For plots with nutrient fertilization, FR was a



218 directly optimized parameter. For our application of the 3-PG model using DA, we removed the
 219 previously simulated dependence of total root allocation on FR(Bryars et al., 2013; Gonzalez-
 220 Benecke et al., 2016). Therefore, plots with lower FR could be interpreted to have lower
 221 quantum yield. Other environmental conditions influenced GPP, including temperature, frosts
 222 days, and vapor pressure deficit with a description of these modifiers found in the Supplemental
 223 Material.

224

225 Each month, net primary production (a parameterized and constant proportion of GPP) was
 226 allocated to foliage, stem (stemwood, stembark, and branches), coarse roots, and fine roots.
 227 Differing from previous applications of 3-PG to loblolly pine ecosystems, we modified the
 228 model to simulate fine roots and coarse roots separately. 3-PG also simulated simple population
 229 dynamics by including stem density as a state variable. Stem density and stem biomass pools
 230 were reduced by both density-dependent and density-independent mortality (a new
 231 modification), with the former based on the concept of self-thinning. Finally, we added a simple
 232 model of hardwood understory vegetation to enable the use of estimates of gross primary
 233 productivity and evapotranspiration from eddy-covariance tower studies with significant
 234 understories. Details of the model can be found in the Supplemental Material.

235

236 The water cycle was a simple bucket model with transpiration predicted using a Penman-
 237 Monteith approach (Bryars et al., 2013; Gonzalez-Benecke et al., 2016; Landsberg and Waring,
 238 1997). The canopy conductance used in the Penman-Monteith subroutine was modified by
 239 environmental conditions. The modifiers include the same available soil water and vapor
 240 pressure deficit modifier as used in the GPP calculation. Maximum canopy conductance



241 occurred when simulated LAI exceeded a parameterized value of leaf area index (LAI).
 242 Evaporation was equal to the precipitation intercepted by the canopy. Runoff occurred when the
 243 available soil water exceeded a plot-specific maximum available soil water. As in prior
 244 applications of 3-PG, available soil water was not allowed take a value below a minimum
 245 available soil water, resulting in an implicit irrigation in very dry conditions.

246
 247 The 3-PG model used in this study simulated the monthly change in eleven state variables per
 248 plot: four stocks for loblolly pines, five stocks for understory hardwoods, loblolly pine stem
 249 density (stems ha⁻¹), and available soil water. The key fluxes that were used for DA included
 250 monthly GPP, monthly evapotranspiration (ET), annual root turnover, and annual foliage
 251 turnover. In total, 46 parameters were required by 3-PG with 31 of the parameters optimized
 252 using DA (Table 1, Supplemental Table 1, SI Table 2). The model required mean daily
 253 maximum temperature, mean daily minimum temperature, daily PAR, total frost days, total rain
 254 at the monthly time scale, monthly atmospheric CO₂, and latitude. Each plot also required
 255 maximum available soil water, site index, mean annual temperature, and the initial condition of
 256 the eleven state variables as model inputs (Figure 2).

257

258 **2.2 Observations**

259 We used thirteen different data streams from 294 plots at 187 unique locations spread across the
 260 region to constrain model parameters (Table 2; Figure 3). The data streams covered the period
 261 between 1981 to 2015. All data streams were not available in all plots (Table 2; Table 3). The
 262 most common set of data streams were annual or less frequent observations of stand stem
 263 biomass (defined as the sum of stemwood, stembark and branches), winter foliage biomass, and
 264 living tree counts. The stem and foliage biomass were optimized using regional allometric



models based on measurements of tree diameter, height, and plot level-stem size distributions (Gonzalez-Benecke et al., 2014). The most comprehensive set of data streams was from Duke Forest where annual measurements and allometric-based estimates were made of stem biomass (loblolly pine and hardwood), coarse root biomass (loblolly pine and hardwood), fine root biomass (combined loblolly pine and hardwood), stem count (loblolly pine only), leaf turnover (combined loblolly pine and hardwood), and fine root production (combined loblolly pine and hardwood). The Duke Forest dataset (DK3 combined with the Duke FACE CO₂ fertilization study) also included monthly observations of LAI, gross ecosystem production (GEP; modeled gross primary productivity from net ecosystem exchange measured at an eddy-covariance tower), and ET. The set of data streams associated with a particular site and experimental design is shown in Table 3. The measurement uncertainty associated with each data stream is listed in Table 2. Since the model used a monthly time-step, and plots with only biomass and stem density observations were more common than plots with monthly flux estimates, the data used in the optimization cost function were not dominated by high frequency data streams (GEP and ET).

2.3 Data assimilation method

We used a hierarchal Bayesian framework to approximate the posterior probability distributions of model parameters in Table 1, the model process uncertainty parameters, and the latent model states and fluxes. The latent model states represented the ‘true’ stock or flux before measurement uncertainty was included in the observation. Our hierarchal approach was designed to partition uncertainty that is attributable to uncertainty in parameters, model process, and measurements (Hobbs and Hooten, 2015). Previous forest ecosystem DA efforts have either focused on parameter uncertainty, by using measurement uncertainty as the variance term in a Gaussian cost



function, or on total uncertainty by directly estimating the Gaussian variance term. The latter combines measurement uncertainty and process uncertainty into the same parameter and is unable to be used for developing prediction intervals, as prediction intervals only include parameter and process errors (Dietze et al., 2013; Hobbs and Hooten, 2015). Here, our focus was on estimating the probability distribution of forest biomass before uncertainty is added through measurement.

294

First, we estimated the probability of a latent state or flux ($z_{i,m,p}$) for each data point (i) from each data stream (m) in a plot (p) using the 3-PG model with the plot FR. This included the optimized parameters (θ_F), fixed parameters (θ_C), soil characteristic inputs (S), climate inputs (C), site index (SI), fertility (FR_p), and initial conditions (I) required by the 3-PG to simulate each plot, $f(\theta_F, \theta_C, C, S, I, FR_p)$. The latent state ($z_{i,m,p}$) was assumed to be normally distributed with the mean from the 3-PG simulation and an optimized, data stream-specific, process variance $\sigma_{m,(process)}^2$

301

$p(\text{process}|\text{process parameters})=$

$P(z_{i,m,p} | f(\theta_F, \theta_C, C, S, I, FR_p), \sigma_{m,(process)}^2)$

$\sim \text{Normal}(z_{i,m,p} | f(\theta_F, \theta_C, C, S, I, FR_p), \sigma_{m,(process)}^2)$

Equation 1

305

The unobserved true state related to the observed state through a data observation model. In the sampling model, the measured state ($y_{i,m,p}$) was a random sample from a normal distribution with a mean of the true state and a data point-specific standard deviation ($\sigma_{i,m,p}^2$).

309

$p(\text{data}|\text{process}, \text{data parameters})=$



$$P(y_{i,m,p} | z_{i,m,p}, \sigma_{i,m,p}^2) \sim \text{Normal}(y_{i,m,p} | z_{i,m,p}, \sigma_{i,m,p}^2) \quad \text{Equation 2}$$

312

313 This standard deviation ($\sigma_{i,m,p}^2$) represented measurement uncertainty and was similar to the
 314 denominator in least-squares approach that is commonly used in DA (Bloom and Williams,
 315 2015; Keenan et al., 2011).

316

317 Each parameter (θ_F) that was optimized using the Bayesian method had a prior probability that is
 318 specified in Table 1. The prior distribution for the standard deviation $\sigma_{m,(process)}^2$ parameters
 319 were uniformly distributed:

320

$$p(\text{process parameters} | \text{priors}) \times p(\text{priors}) = P(\sigma_m^2) \times P(\theta_F) \quad \text{Equation 3}$$

322

323 where

324

$$P(\sigma_m^2) \sim \text{unif}(0.001, 100) \quad \text{Equation 4}$$

326

327 and

328

$$P(\theta_F) \sim \text{See Supplemental Table 1} \quad \text{Equation 5}$$

330

331 Finally, following the description of the plot specific FR_p described above, the probability for
 332 fertilized treatments was based on a comparison to the control treatment FR.

333



$$P(FR_p | \theta_F, E) = \begin{cases} 1 & \text{if non-fertilized} \\ 1 & \text{if fertilized and } FR_p \geq FR \text{ of control plot} \\ 0 & \text{if fertilized and } FR_p < FR \text{ of control plot} \end{cases} \quad \text{Equation 6}$$

335

336 Our complete Bayesian model for estimating the posterior distributions for the parameters (θ_F),
 337 process uncertainty ($\sigma_{m,(process)}^2$), and unobserved true states ($z_{i,m,p}$) was:

338

$$P(\theta_F, \sigma_m^2, z_{i,m,p} | y_{i,m,p}, \sigma_{i,m,p}^2, \theta_C, S, C, SI, I) \propto$$

$$P(z_{i,m,p} | f(\theta_F, \theta_C, FR_p, E), \sigma_m^2) P(y_{i,m,p} | z_{i,m,p}, \sigma_{i,m,p}^2) P(FR_p | \theta_F, E) P(\theta_F) P(\sigma_m^2) \quad \text{Equation 7}$$

341

342 We numerically estimated the posterior distributions using the Monte-Carlo Markov Chain –
 343 Metropolis Hasting (MCMC-MH) algorithm (Zobitz et al., 2011). This approach has been widely
 344 used to approximate parameter distributions in ecosystem DA research (Fox et al., 2009;
 345 Trudinger et al., 2007; Williams et al., 2005; Zobitz et al., 2011). We adapted the size of the
 346 jump for each parameter (i.e., how far a proposed new value can potentially be from the current
 347 value) to ensure the acceptance rate of the parameter set is between 22% and 43% (Ziehn et al.,
 348 2012). All MCMC-MH chains were run for 30 million iterations with the first 15 million
 349 iterations discarded as the burn-in. Three chains were run and compared for convergence and we
 350 sampled every 1000th parameter in the final 15 million iterations of the MCMC-MH chain. This
 351 thinned chain was used in the analysis described below. The 3-PG model and MCMC-MH
 352 algorithm were programed in FORTRAN 90 and used OpenMP to parallelize the simulation of
 353 each plot within an iteration of the MCMC-MH algorithm.

354



355 **2.4 Model simulations**

356 Each plot simulated required initial conditions for each model state, climate inputs, soil
357 characteristic inputs, and site index. We used the first observation at the plot as the initial
358 conditions for the loblolly pine vegetation states (foliage biomass, stem biomass, coarse root
359 biomass, fine root biomass, and stem number). When observations of coarse biomass and fine
360 root biomass were not available, these stocks were initialized as a mean region-wide proportion
361 of the observed stem biomass. However, the value of initial root biomass in plots without
362 observations was not important because the plots without root observations did not contribute to
363 the root cost function and root biomass does not influence any other functions in the model. In
364 the two plots with flux observations (US-Dk3 and US-NC2), hardwood understory was also
365 initialized using the first set of observations. Initial fine root and coarse biomass was distributed
366 between loblolly pine and hardwoods based on their relative contribution of total initial foliage
367 biomass. The initialized available soil water was assumed to be equal to the maximum available
368 soil water because most plots were initialized in winter months when plant demand for water is
369 minimal. The maximum available soil water in each plot was extracted from the SSURGO soils
370 dataset (Staff, 2016). We assumed that the minimum available soil water was zero. The value we
371 used corresponded to the maximum available soil water for the top 1.5 m of the soil. Because we
372 focused on a region-wide optimization, we used region-wide 4-km estimates of observed
373 monthly meteorology as inputs and to collect the 35-year mean annual temperature for each plot
374 (Abatzoglou, 2013). Site index was based on height measurements at age 25 in each plot or
375 calculated by combining observations of height at younger ages with an empirical model



376 (Dieguez-Aranda et al., 2006).

377

378 We simulated the experiments by altering the environmental modifiers or by modifying the
379 environmental inputs. Nutrient addition experiments were simulated by directly estimating FR,
380 rather than calculating from Equation 2, and by requiring the optimized FR in the fertilized plot
381 to be equal to or greater than the FR in the control plots. Throughfall exclusion experiments were
382 simulated by decreasing rain inputs by 30% in the treatment plots. This assumed that the
383 fractional reduction in precipitation and throughfall were equal. The SETRES Irrigation
384 experiments were simulated by adding 650 mm to precipitation between April and October. CO₂
385 enrichment experiments were simulated by setting the atmospheric CO₂ input equal to the
386 treatment mean from the elevated CO₂ rings (570 ppm). While not an experiment, one plot (US-
387 NC2) included a thinning treatment during the period of observation. We simulated the thinning
388 by specifying a decrease in the stem count that matched the proportion removed at the site, with
389 the biomass of each tree equivalent to the average of trees in the plot.

390

391 **2.4 Model experiments and analysis**

392 Our analysis focused on comparing parameter distributions and predictions among simulations
393 that used different experimental treatments to estimate the posterior distributions (Table 4). To
394 examine the influence of the Duke FACE CO₂ fertilization, we compared a one stage vs. a two-
395 stage data assimilation process. The one stage process assimilated all observations in all plots
396 and experiments simultaneously. In this approach, the elevated CO₂ plots only represented 5 of
397 the 294 plots across the region and thus a relatively minor contribution to the likelihood (cost-
398 function) calculation. The two-stage process used the observations from Duke FACE, US-Dk3



399 flux site, the other flux site in North Carolina (US-NC2) to estimate parameter posteriors using
 400 the priors in Table 1 and SI Table 1. These sites were grouped together because they were the
 401 most data rich, had the high frequency data streams (monthly GEP, ET, and LAI), and were
 402 relatively close in geography. FR was directly estimated for all plots in the first stage, with the
 403 FR of a fertilized plot required to be equal to or higher than its control plot. The FR of the CO₂
 404 experiment was equal to the corresponding control plot estimated FR. The FR of the control plot
 405 was required to be greater than 0 and, if associated with a nutrient fertilization plot, less than the
 406 FR of the fertilized plot.

407

408 For the second DA stage, the posterior distributions from the first stage were used as priors for
 409 the assimilation of the region-wide observations from the PINEMAP, FPC RW 18, FMRC
 410 Thinning, SETRES, and Waycross studies (Table 4). We compared the CO₂ quantum yield
 411 enhancement parameter (Calpha700) between the one and two stage approaches to evaluate how
 412 the estimation of CO₂ fertilization of plant growth depended on how the Duke FACE data are
 413 used in data assimilation. We also estimated the distribution of the percentage increase in net
 414 primary productivity (NPP) associated with the elevated CO₂ treatment using the one and two
 415 stage data assimilation approaches. The distribution of the percentage increase in NPP was
 416 calculated by randomly selecting 1000 parameter sets, with replacement, from the 1-stage
 417 converged MCMC chains. This calculation was repeated using the 2-stage approach.

418

419 Based on the results from comparing the one and two stage approaches (see results below), we
 420 proceeded using the two-stage approach to examine the influence of the water manipulation and
 421 nutrient fertilization experiments on posterior distributions and predictions. To evaluate the



422 influence of water manipulation experiments, we repeated the second stage of the data
423 assimilation without the plots where water was added or subtracted. To evaluate the influence of
424 the nutrient manipulation experiments, we first repeated the first stage of data assimilation
425 without the nutrient addition plots in the Duke FACE experiment and used those posteriors as
426 priors to the second stage. This ensured that the priors to the second stage of data assimilation
427 did not include information from nutrient addition experiments. The second stage then excluded
428 the other nutrient manipulation experiments in the region.

429

430 To examine how the exclusion of the water manipulation experiments influenced parameter
431 inference and predictions, we first examined how the parameter distributions changed from
432 initial priors through the two assimilation stages. With respect to the water manipulation
433 experiments, we focused on the shape of the relationship between available soil water and the
434 quantum yield and stomatal conductance modifier (governed by parameters SW1 and SW2) with
435 and without assimilating the water manipulation experiments. To illustrate the capacity to
436 estimate the probability distribution of predictions using the posterior uncertainty in parameters,
437 we analyzed a focal site in Georgia, near the center of the loblolly pine range (circle in Figure 2).
438 At the focal site, we predicted the sensitivity of stem biomass at age 25 (hereby referred to as
439 STEM₂₅) to a 30% increase and a 30% decrease in annual precipitation with and without
440 assimilating the water experiments. A 30% percent decrease in precipitation mirrors the
441 magnitude of reduction in the experimental throughfall reduction studies used in DA (Table 3
442 and Figure 3). Our prediction distributions were calculated by integrating across the parameter
443 uncertainty by repeating simulations using 1000 random draws from the converged chain of the
444 posteriors. Finally, we predicted the regional response to a reduction in precipitation from



445 historical using the median posterior parameter values from the data assimilation with and
 446 without the water experiments included. Our regional corresponded to the native range of
 447 loblolly and used the HUC12 (USGS 12-digit Hydrological Unit Code) watershed as the scale of
 448 simulation. For each HUC12 in the region we used the mean site index, 30-year mean annual
 449 temperature, available soil water aggregated to the HUC12 level, and monthly meteorology as
 450 inputs (Figure 2). We simulated forest development from 1989 to 2014 using actual precipitation
 451 and again with a 30% reduction in precipitation. We focused our analysis on the percent change
 452 in $STEM_{25}$ between the two simulations.

453

454 To examine how the exclusion of the nutrient addition experiment influenced parameter
 455 inference and prediction, we focused on the difference in maximum quantum yield parameter (α)
 456 and the relationship between site index and soil fertility modifier (FR) with and without
 457 assimilating the nutrient experiments. Additionally, we simulated how stem biomass at age 25
 458 ($STEM_{25}$) responded to a complete removal of nutrient limitation (FR = 1) for the focal site in
 459 Georgia. As in the precipitation sensitivity described above, we represented the percentage
 460 change in $STEM_{25}$ between simulations with estimated FR and FR = 1 as a distribution by
 461 integrating across parameter uncertainty. We predicted the regional response to nutrient
 462 fertilization by setting the FR at all HUC12 units (see previous paragraph) equal to 1 using the
 463 median posterior parameter values from data assimilation where nutrient addition experiments
 464 were either included or not. We focused on the regional pattern in the percentage change in stem
 465 biomass with the predicted FR (current level fertility) and FR = 1 (nutrient limitation removed).

466

467 Finally, we assessed overall model performance of the 2-stage approach for data assimilation



with all experimental types included in DA, excluding the nutrient addition experiments, and
 excluding the nutrient addition experiments using an out-of-sample approach. The approach held
 40 random FMRC thinning study plots (Table 3) out from the assimilation, predicted the 40 plots
 using the median parameter values, and compared the predicted stem biomass to the observed
 stem biomass. These were plots without any manipulations of nutrients or water, were located
 throughout the region, and had measurement ages up to 30 years old. For each plot, we only used
 the most recent observed values to increase the time length between initialization and validation.
 We repeated the validation for four unique sets of 40 FMRC thinning study plots.

476

3 Results

Our multi-site, multi-experiment, multi-data stream DA approach was able to constrain most
 parameters in the 3-PG model (31 of 46 parameters were optimized; Table 6; Supplemental
 Table 3; Supplemental Figure 1-3). The 31 optimized parameters were the most sensitive
 parameters in the 3-PG model, defined by the change in total biomass at age 25 for the focal site
 in Georgia to a 10% change in the parameter (Table 1; Supplemental Table 1). One exception
 was the light extinction coefficient (k), which showed high sensitivity but was assumed to be
 fixed because it strongly co-varied with the quantum yield parameter (α). Parameters associated
 with biomass allocation had priors with large variance but DA was able to provide posteriors
 with relatively low variance (pFS2, pFS20, pR, and pCRS; Supplemental Figure 1; Supplemental
 Table 3). The DA process also produced posterior distributions that had less variability than the
 prior distribution for the important parameters associated with light-use efficiency (α , y , FR1,
 and FR2; Table 5). DA did not change the parameter distributions, i.e., the posterior and prior
 distributions were similar, for the parameters that governed the temperature sensitivity of



quantum yield, the VPD sensitivity of quantum yield, and the maximum canopy conductance
 (Supplemental Figure 1-2; Supplemental Table 3). These parameters had strong priors supported
 by previous research on loblolly pine physiology. Finally, the DA approach was able to estimate
 the distributions of the process uncertainty parameters (Supplemental Figure 3; Supplement
 Table 4).

496

The addition of the second stage of assimilation that used region-wide observations and
 posteriors from the DK+NC2 assimilation modified the distributions of the parameters that
 related to allocation and mortality but did not provide additional constraint on the physiological
 parameters (Table 5). In particular, the parameters associated with the self-thinning curve and
 allocation of coarse roots had non-overlapping 95% credible intervals between the DK+NC2 and
 RW assimilation. The larger estimate for W_{sx1000} and lower value for $thinPower$ in the
 DK+NC2 indicated self-thinning was lower at the sites in the DK+NC2 assimilation than the
 average of the other sites in the region. The lower value for the $pCRS$ parameter indicated that
 less NPP was allocated to coarse roots in the DK+NC2 assimilation than the RW assimilation.

506

The two-stage assimilation was critical for constraining the CO_2 quantum yield enhancement
 parameter ($f_{\alpha 700}$). Both the mean of the posterior distribution and the range of the 95%
 credible interval were smaller for $f_{\alpha 700}$ when all observations were assimilated
 simultaneously (1-stage approach) than the distribution estimated using the 2-stage approach
 (Duke and NC2 assimilated before the region-wide assimilation) (Figure 5a; Table 5). Despite
 the same data used in both approaches, the differences in $f_{\alpha 700}$ led to a predicted lower
 enhancement of NPP associated with elevated CO_2 in the experiment. The 1-stage assimilation



514 approach had a median increase in NPP between the control and elevated CO₂ treatments of 15%
 515 compared to a 27% in the two-stage approach (Figure 5b).

516

517 The RW assimilation constrained the soil fertility parameters that were necessary to enable
 518 regional simulations. Our regional model using the 2-stage approach performed well compared
 519 to stem biomass data not used in the assimilation. The mean bias in stem biomass of the four out-
 520 of-sample validation sets was -6.7 % and the RMSE was 21.2 Mg ha⁻¹ (Figure 4).

521

522 Excluding the nutrient addition experiments from the DA increased the simulated level of
 523 nutrient limitation but did not change the predictive capacity of the independent non-manipulated
 524 validation set. DA without nutrient fertilization experiments had a greater and more uncertain
 525 value for the maximum quantum yield parameter (α ; Figure 6a; Table 5). This parameter was
 526 shared across all plots and modified by the environmental conditions at each plot. To compensate
 527 for the higher α parameter when nutrient fertilization experiments were excluded from DA, the
 528 two soil fertility parameters (FR1 and FR2) combined to predict a 10% lower FR values for a
 529 given site index and mean annual temperature (Figure 6b). Subsequently, the prediction for the
 530 percentage change in STEM₂₅ associated with maximum fertilization (i.e., setting FR = 1) at the
 531 focal site in Georgia was 7% higher and had greater uncertainty when nutrient fertilization
 532 experiments were excluded from the DA (Figure 6c). The RMSE and mean bias of the non-
 533 manipulated validation set was 20.4 Mg ha⁻¹ and -4.8 %, respectively (SI Figure 1a)

534

535 Excluding the water manipulation experiments from the DA reduced the sensitivity to available
 536 soil water but, similar to the inclusion of the nutrient addition experiments, did not change the



537 predictive capacity of the independent non-manipulated validation set. The combined differences
 538 in the SW1 and SW2 parameters between the DA with and without the water manipulation
 539 experiments decreased the sensitivity of quantum yield and canopy conductance to a reduction in
 540 available soil water (Figure 7a). For example, at an available soil water to maximum available
 541 soil water ratio of 0.50, the quantum yield and canopy conductance modifier decreased from 0.95
 542 without water experiments to 0.8 with water experiments (Figure 7a). At the focal site in
 543 Georgia, the sensitivity of STEM₂₅ to a reduction in annual precipitation (Figure 7b) was larger
 544 when the water experiments were included in the DA (-8.5% median change in STEM₂₅ for a
 545 30% reduction in precipitation) than when the experiments were excluded (-4.1% median change
 546 in STEM₂₅ for a 30% reduction in precipitation). Similarly, the predictions of STEM₂₅ change
 547 associated with a 30% increase in precipitation (median: 3.8%) were higher when water
 548 experiments were included than when not included (median: 1.1%). The magnitude of
 549 uncertainty in the predictions did not differ substantially between forecasts with and without
 550 water experiments (Figure 7b). The RMSE and mean bias of the non-manipulated validation set
 551 was 19.3 Mg ha⁻¹ and -5.8 %, respectively (SI Figure 1b)

552

553 Regionally (i.e., the native range of loblolly pines), using the two-stage approach (RW), the most
 554 productive areas were the coastal plains and the interior of Mississippi and Alabama (Figure 8).
 555 These patterns were largely driven by patterns in the soil fertility factor (FR; Figure 9), reflecting
 556 the sensitivity of the 3-PG model to the FR parameters (Table 1). The area weighted mean
 557 STEM₂₅ response to fertilization (represented by setting FR = 1) across the region was 28% with
 558 the highest response occurring in the far west of the region, the Piedmont of Georgia, the interior
 559 of the gulf coast, and the northern reach of the region (Figure 10a). These were all areas with the



lowest soil fertility parameter. The least responsive region to nutrient addition was in Florida (Figure 10a). Excluding the nutrient addition experiments from the DA increased the sensitivity to nutrient addition (Figure 10b), as shown for the focal Georgia site (Figure 6b), but did not change the spatial patterns of the response.

The sensitivity of forest production to a 30% reduction in precipitation varied across the region. The most sensitive areas, the Piedmont of Georgia and the western edge of the region, predicted up to a 13.1% decline in $STEM_{25}$ (Figure 11a). These were warm areas with relatively low precipitation before the 30% reduction (Figure 2c). The least sensitive area was the interior of the gulf coast (<1% decline; Figure 11a), the area with the highest precipitation in the region (Figure 2c). The regional mean reduction in $STEM_{25}$ associated with a 30% decrease in precipitation was 5.7% (Figure 11a). Excluding the water manipulation experiments from DA reduced the regional mean sensitivity to 1.7% (Figure 11b).

4 Discussion

Using DA to parameterize models applied to forecasting ecosystem change requires detangling the vegetation responses to temperature, precipitation, nutrients, and elevated CO_2 . To address this challenge, we introduced a regional-scale hierarchical Bayesian approach (DAPPER) that assimilated data across environmental gradients and ecosystem manipulation experiments into a modified version of the 3-PG model to estimate parameters and generate uncertainty estimates on predictions of carbon and water cycling across the whole native range of loblolly pine. Furthermore, we organized observations of carbon stocks, carbon fluxes, water fluxes, vegetation



583 structure, and vegetation dynamics that spanned 35 years of forest research (Figure 3; Table 3) in
584 a region with large and dynamic carbon fluxes (Lu et al., 2015). By combining the DAPPER
585 system with the regional set of observations, we were able to estimate parameters in a model
586 with high predictive capacity (Figure 4) and with quantified uncertainty on parameters (Table 5).
587 We also found that the predictions of forest productivity response to rising CO₂, altered
588 precipitation, and altered nutrient availability were highly sensitive to the types of experiments
589 used in DA as well as the methodological approach applied.

590

591 We found that including nutrient and water manipulation experiments aided in distinguishing the
592 mechanisms driving patterns in biomass across the region. Including these experiments in the
593 data-assimilation did not improve the predictive capacity of the independent validation set of
594 non-manipulation plots. However, including nutrient and water manipulation did change the
595 underlying mechanisms explaining the patterns in stem biomass. Without the nutrient and water
596 manipulation experiments, the same biomass predictions were attributable to a higher level of
597 nutrient limitation and a lower level of water limitation. This resulted in differing sensitivities to
598 changes in nutrient or water availability. Overall, this finding highlights a key challenge when
599 parameterizing ecosystem models that will be used for global change predictions, that different
600 combinations of environmental drivers can produce similar predictions of current observations.
601 Ecosystem manipulation experiments are an important tool for addressing this challenge.

602

603 Parameter and process identifiability, or equifinality, presents a challenge when parameterizing
604 ecosystem models using DA (Luo et al., 2009). One important source of equifinality is the
605 tradeoff between parameters governing the potential productivity of the vegetation and the



606 downregulation of productivity due to nutrient limitation. When using observational data at a
607 single site, a single parameter is often optimized to set a photosynthetic rate per absorbed light,
608 i.e., a quantum yield. This single parameter combines the potential photosynthesis set by climate
609 and the influence of nutrient limitation on photosynthesis into a single parameter. However,
610 separating these two processes into two or more parameters is challenging because a high
611 potential quantum yield parameter (α) and high nutrient limitation (FR) can mathematically yield
612 the same photosynthetic rate as low potential quantum yield and low nutrient limitation. The
613 former implies a larger potential response to nutrient addition than the latter. We found that
614 including nutrient addition experiments in DA helped overcome this challenge. In the case of the
615 3-PG model used in this study, the maximum quantum parameter (α) and soil fertility parameters
616 (FR1 and FR2) were more constrained and inferred lower levels of nutrient limitation across the
617 region when nutrient fertilization experiments were included in the DA. This finding likely
618 extends to other models that include the concept of potential productivity and productivity
619 downregulated by nutrient limitation. For example, the applications of the Data Assimilation
620 Link Ecosystem Carbon (DALEC) model (Williams et al., 2005) to DA often assumed nine of
621 the ten parameters associated with photosynthesis were fixed, thus using a single parameter to
622 represent both the quantum yield (defined as nitrogen use efficiency in DALEC) and the
623 magnitude of nitrogen limitation of a site (Fox et al., 2009). The use of a single parameter, rather
624 than using nutrient addition experiments to separate into multiple parameters, is appropriate
625 when assuming nutrient availability is static. Applications of DA to predictions of ecosystems
626 with changing nutrient availability, either through management, elevated CO₂, or nitrogen
627 addition, would benefit from using nutrient addition studies to quantify the magnitude of nutrient
628 limitation. Studies of known nutrient gradients could be used in lieu of nutrient addition studies,



629 but effort must be made to account for confounding abiotic factors, such as available soil water
630 or climatic conditions, that may co-vary with nutrient availability.
631
632 Another challenge in DA is deciding how to weigh different types of data used in model fitting
633 (Gao et al., 2011; Wutzler and Carvalhais, 2014). Here we demonstrate that DA efforts should
634 also consider how to weigh different types of ecosystem experiments. In our analysis, we
635 included three types of experiments: nutrient addition, water manipulation, and CO₂ fertilization.
636 The nutrient addition and water manipulation experiments were represented by multiple sites
637 across the region while the CO₂ fertilization only occurred at a single location (Figure 3). We
638 found that the parameter that represents the increase in maximum quantum yield under elevated
639 CO₂ was substantially lower when all observations, sites, and experiments were assimilated
640 simultaneously than when the CO₂ fertilization experiment was given greater weight. The greater
641 weight was applied by first assimilating the CO₂ fertilization experiment and using the posteriors
642 as priors for assimilating the remaining observations. Providing additional weight on the single
643 site with unique environmental conditions (i.e., atmospheric CO₂ at 570 ppm) using a two-stage
644 data-assimilation, we were able to more accurately represent the observed differences in NPP
645 between the ambient and elevated CO₂ treatments at the Duke site (McCarthy et al., 2010).
646 Given that only a few of the parameters were significantly different between the Duke site and
647 the other studies across the region, it may be possible to optimize one parameter for the Duke site
648 and another parameter for the other studies in a 1-stage approach that combines all the plots into
649 a single assimilation. However, the 2-stage approach was required to identify which parameters
650 were different between the Duke site and the other studies. Overall, we suggest that DA efforts
651 using multiple studies and multiple experiment types identify whether particular experiments at



652 limited number of sites have the potential to uniquely constrain specific parameters. In this case,
653 additional weight may be needed to avoid having the signal of the unique experiment
654 overwhelmed by the large amount of data from the other sites and experiments.
655
656 Our analysis highlights that nutrient limitation of productivity was widespread across the region.
657 The largest potential gains in productivity from nutrient addition were predicted in central
658 Georgia, an area with warm annual temperatures but poor soils, as expressed in the low site
659 index. The baseline fertility used in our regional analysis was derived from an empirical model
660 of site index that was developed using field plots with minimal management (Sabatia and
661 Burkhardt, 2014). Subsequently our estimate of baseline fertility is likely on the low end of forest
662 stands currently in production. Further, we recognize that the site index model had uncertainty
663 that could be formally incorporated into the hierarchical Bayesian approach in future applications.
664
665 The soil fertility modifier has commonly been used to calibrate the 3-PG for applications to a
666 single site, with recent work focused on developing an approach to predicting the soil fertility
667 modifier from environmental conditions (Gonzalez-Benecke et al., 2016; Subedi et al., 2015).
668 We have extended prior efforts to develop a simple predictive model of FR in two ways. First,
669 we simultaneously calibrated the parameters in the empirical FR model alongside the other
670 parameters in the 3-PG model. Prior studies have assumed fixed values for the 3-PG model
671 parameters, fitted FR for plots with observations, and developed a relationship between FR and
672 site index. Our Bayesian approach to simultaneously calibrating the 3-PG parameters and the FR
673 model allowed for the estimation of uncertainty and covariation among parameters in the 3-PG
674 and FR models. Second, we included a climate term (mean annual temperature) in the



relationship between site index and FR. This resulted in a lower FR for a given site index in warmer locations. By including the climate term, FR can be interpreted as relative to the climate at a given location and the potential productivity of a plot can be optimized by setting FR equal to 1. When a climate term is not used in the empirical FR model, FR is relative to the greatest site index in the region, which does not occur in the northern extent of the region even in fertilized plots due to climatic constraints.

681

Our simulations show that loblolly pine productivity was not strongly sensitive to changes in precipitation at present day temperatures and atmospheric CO₂. We simulated a 30% reduction in annual precipitation and found a maximum of a 13.1% reduction in productivity. A 30% reduction in precipitation is plausible but is more extreme than most Multivariate Adaptive Constructed Analogs (MACA) downscaled climate model projections for the Representative Concentration Pathway (RCP) 8.5 scenario from the CMIP5 Project (comparing the 1971-2000 period to the 2070-2099) (Abatzoglou and Brown, 2012; Taylor et al., 2012). Central Georgia was the most responsive to precipitation reduction, paralleling the spatial patterns in the response to nutrient addition, suggesting that the region is able to support high productivity but is sensitive to nutrient and precipitation levels. The simulated sensitivity was likely due to poor soils (low site index) and low baseline precipitation relative to the warm climate. Our predictions of low sensitivity to precipitation reduction or addition were derived from assimilating observations from throughfall exclusion and irrigation experiments across the region. Prior publications from the studies used in DA also reported low sensitivities to water manipulations, indicating that our predictions are likely not biased (Albaugh et al., 2004; Samuelson et al., 2014; Ward et al., 2015; Wightman et al., 2016). For example, the throughfall exclusion experiment at the focal site in



698 Georgia, reported a 13% reduction in stem production during a dry year but a 0% reduced during
699 a wet year, resulting in a 7% reduction of productivity over a 2-year period in response to a 30%
700 reduction in throughfall (Samuelson et al., 2014). Our predicted 8.5% reduction to a 30%
701 reduction in precipitation compares well to the observed change, noting that our sensitivity
702 integrated over a 25-year rotation and included a mix of relatively wet and dry years.

703

704 The 3-PG model included a highly simplified representation of interactions between the water
705 and carbon cycles that resulted in parameterizations that, while consistent with observations, may
706 contain assumptions that require additional investigation. For example, transpiration is modeled
707 as a potential canopy transpiration that occurred if leaf area was not limiting transpiration. The
708 LAI at which leaf area was no longer limiting was a parameter that was optimized (LAI_{gex} in SI
709 Table 3), resulting in a value of 2.3. Interestingly, this optimized value is consistent with the
710 scant literature on this topic. In their analysis of multi-year measurements of transpiration in
711 loblolly pine, Phillips and Oren (2001) observed that transpiration per unit leaf area was
712 relatively insensitive to increases in leaf area above LAI of approximately 2.5. Iritz and Lindroth
713 (1996) reviewed transpiration data from a range of crop species and found only small increases
714 in transpiration above LAI of 3-4. These authors suggest that the threshold-type responses
715 observed were related to the range of LAI at which self-shading increases most rapidly, therefore
716 limiting increases in transpiration. The resulting model behavior of "flat" transpiration above 2.3
717 LAI, with gradually decreasing photosynthesis above that value, results in increasing water use
718 efficiency at higher LAI values. The parameterization of the relationships between transpiration
719 and photosynthesis in 3-PG would likely benefit from additional data beyond the two eddy-
720 covariance studies with ET observations used here. For example, canopy conductance estimates,



721 and their associated uncertainty have been derived from assimilating observations from sap-flow
722 measurements into a model that scales from the sensor measurements to canopy transpiration
723 using LAI observations (Bell et al., 2015). This sap-flow to canopy conductance scaling
724 approach (the State Space Canopy Conductance (StaCC) model (Bell et al., 2015)) produces a
725 probability distribution of monthly canopy conductance that could be integrated into the
726 DAPPER system by treating the posterior estimates of StaCC as the distribution of the data in
727 equation 2. Second, the optimized parameters that described the relationship between relative
728 available soil water and the modifier of photosynthesis and transpiration predicted a modifier
729 value greater than zero when the relative available soil water was zero. This resulted in positive
730 values from photosynthesis and transpiration when the average available soil water during the
731 month was zero. In practice, the monthly available soil water was rarely zero during simulations,
732 which presents a challenge constraining the shape of the available soil water modifier. The priors
733 for the two available soil moisture modifiers (SW1 and SW2) had ranges that permitted the
734 modifier to be zero. Therefore, additional data is likely needed during very dry conditions to
735 develop a more physically based parameterization. Alternatively, the parameterization of a non-
736 zero soil moisture modifier at zero available soil water may be due to trees having access to
737 water at soil depths deeper than the top 1.5 m of soil represented by the bucket in 3-PG. Overall,
738 it is important to view the parameterization presented here as a phenomenological relationship
739 that is consistent with observations from throughfall exclusion and irrigation experiments as well
740 as observations across regional gradients in precipitation.

741

742 Beyond the specifics of the 3-PG modeling efforts, the DA of regional observations into a
743 monthly, computationally tractable ecosystem model can potentially inform Earth system



744 modeling efforts. While the details of physiology differ between 3-PG and global land-surface
 745 models, the concepts governing NPP allocation are similar. Therefore, DA using the 3-PG model
 746 can be used to parameterize the allocation patterns of similar plant types in a global model. One
 747 land-surface model, the Community Land Model (CLM), includes parameters that govern the
 748 ratio of stem to leaf allocation, ratio of coarse root to stem allocation, and the ratio of leaf to fine
 749 root allocation, parameters that are also optimized in DAPPER. As an example, the ratio of fine
 750 root to leaf allocation in CLM 4.0 and 4.5 for temperate pine plant function type is set to 1,
 751 resulting in equal annual allocation of carbon to foliage and fine roots (Oleson et al., 2013). In
 752 contrast, we found that the median ratio of fine root to foliage allocation was substantially lower
 753 at 0.13 (Table 6). Therefore, simulations in the CLM with the lower value of root allocation
 754 would have higher allocation to aboveground tissues if the loblolly pine parameters from our
 755 analysis were used. This would increase carbon accumulation in woody tissues and could alter
 756 predictions of nutrient limitation because stems have higher C:N ratios. Other parameters,
 757 including the stem to coarse root ratio, are closer to the values used in the CLM.

758

759 **5 Conclusions**

760 DA is increasingly used for ecological forecasting due to its ability represent prior knowledge,
 761 integrate observations into the parameterization, and estimate multiple components of
 762 uncertainty, including observation, parameter, and process representation uncertainty (Dietze et
 763 al., 2013; Luo et al., 2011b; Niu et al., 2014). Our application of DA to loblolly pine plantations
 764 of the southeastern U.S demonstrated that these ecosystems are well suited as a test-bed for the
 765 development of DA techniques, particularly techniques for assimilating ecosystem experiments.
 766 Further, we found that assimilating ecosystem manipulative experiments into a simple ecosystem



767 model changed predictions quantifying how forest productivity responds to environmental
768 change, highlighting the importance of networks of ecosystem manipulation experiments for
769 helping to parameterize and evaluate ecosystems models (Medlyn et al., 2015).

770

771 **6 Data availability**

772 Observations used in the DA can be found in the following: Duke FACE study can be found in
773 McCarthy et al. (McCarthy et al., 2010), the PINEMAP studies are available through the TerraC
774 database (<http://terrac.ifas.ufl.edu>), the DK3 eddy-flux tower data are available through the
775 Ameriflux database (<http://ameriflux-data.lbl.gov>) , the Waycross data can be found in Bryars et
776 al. (2003), the NC2 data are available upon request with Asko Noormets, the FMRC and FPC are
777 available through membership with the cooperatives. The parameter chains and 3-PG are
778 available upon request from R. Quinn Thomas.

779

780 **Acknowledgments**

781 Funding support came from USDA-NIFA Project 2015-67003-23485 and the Pine Integrated
782 Network: Education, Mitigation, and Adaptation project (PINEMAP), a Coordinated
783 Agricultural Project funded by the USDA National Institute of Food and Agriculture, Award
784 #2011-68002-30185. Additional funding support came from USDA-NIFA McIntire-Stennis
785 Program. The Virginia Space Grant Consortium Graduate STEM Research Fellowship Program
786 provided partial support for A. Jersild. Computational support was provided by Virginia Tech
787 Advanced Research Computing. This research was also supported by grants from the French
788 Research Agency (MACACC ANR-13-AGRO-0005 and MARIS ANR-14-CE03-0007). We
789 thank Luke Smallman and Mat Williams for helpful discussions about data assimilation. We



790 thank the corporate and government agency members of the FPC and FMRC research
 791 cooperatives for supporting the extensive long-term experimental and observational plots in
 792 those datasets.
 793

794 **References**

- 795
 796 Abatzoglou, J. T.: Development of gridded surface meteorological data for ecological
 797 applications and modelling, *International Journal of Climatology*, 33(1), 121–131,
 798 doi:10.1002/joc.3413, 2013.
- 799 Abatzoglou, J. T. and Brown, T. J.: A comparison of statistical downscaling methods suited for
 800 wildfire applications, *International Journal of Climatology*, 32(5), 772–780,
 801 doi:10.1002/joc.2312, 2012.
- 802 Albaugh, T. J., Albaugh, J. M., Fox, T. R., Allen, H. L., Rubilar, R. A., Trichet, P., Loustau, D.
 803 and Linder, S.: Tamm Review: Light use efficiency and carbon storage in nutrient and water
 804 experiments on major forest plantation species, *Forest Ecol Manag*, 376, 333–342,
 805 doi:10.1016/j.foreco.2016.05.031, 2016.
- 806 Albaugh, T. J., Allen, H. L. and Kress, L. W.: Root and stem partitioning of *Pinus taeda*, *Trees*,
 807 20(2), 176–185, doi:10.1007/s00468-005-0024-4, 2005.
- 808 Albaugh, T. J., Lee Allen, H., Dougherty, P. M. and Johnsen, K. H.: Long term growth responses
 809 of loblolly pine to optimal nutrient and water resource availability, *Forest Ecol Manag*, 192(1),
 810 3–19, doi:10.1016/j.foreco.2004.01.002, 2004.
- 811 Albaugh, T., Fox, T., Allen, H. and Rubilar, R.: Juvenile southern pine response to fertilization is
 812 influenced by soil drainage and texture, *Forests*, 6(8), 2799–2819, doi:10.3390/f6082799, 2015.
- 813 Allen, C. B., Will, R. E. and Jacobson, M. A.: Production efficiency and radiation use efficiency
 814 of four tree species receiving irrigation and fertilization, *Forest Science*, 51(6), 556–569, 2005.
- 815 Bartkowiak, S. M., Samuelson, L. J., McGuire, M. A. and Teskey, R. O.: Fertilization increases
 816 sensitivity of canopy stomatal conductance and transpiration to throughfall reduction in an 8-
 817 year-old loblolly pine plantation, *Forest Ecol Manag*, 354, 87–96,
 818 doi:10.1016/j.foreco.2015.06.033, 2015.
- 819 Bell, D. M., Ward, E. J., Oishi, A. C., Oren, R., Flikkema, P. G. and Clark, J. S.: A state-space
 820 modeling approach to estimating canopy conductance and associated uncertainties from sap flux
 821 density data, edited by D. Whitehead, 35(7), 792–802, doi:10.1093/treephys/tpv041, 2015.
- 822 Bloom, A. A. and Williams, M.: Constraining ecosystem carbon dynamics in a data-limited
 823 world: integrating ecological “common sense” in a model–data fusion framework,
 824 *Biogeosciences*, 12(5), 1299–1315, doi:10.5194/bg-12-1299-2015, 2015.



- 825 Bryars, C., Maier, C., Zhao, D., Kane, M., Borders, B., Will, R. and Teskey, R.: Fixed
826 physiological parameters in the 3-PG model produced accurate estimates of loblolly pine growth
827 on sites in different geographic regions, *Forest Ecol Manag*, 289, 501–514,
828 doi:10.1016/j.foreco.2012.09.031, 2013.
- 829 Burkhardt, H. E., Cloeren, D. C. and Amateis, R. L.: Yield relationships in unthinned loblolly pine
830 plantations on cutover, site-prepared lands, *Southern Journal of Applied Forestry*, 9(2), 84–91,
831 1985.
- 832 Carlson, C. A., Fox, T. R., Allen, H. L., Albaugh, T. J., Rubilar, R. A. and Stape, J. L.: Growth
833 responses of loblolly pine in the Southeast United States to midrotation applications of nitrogen,
834 phosphorus, potassium, and micronutrients, *Forest Science*, 60(1), 157–169,
835 doi:10.5849/forsci.12-158, 2014.
- 836 DeLucia, E. H., Drake, J. E., Thomas, R. B. and Gonzalez-Meler, M.: Forest carbon use
837 efficiency: is respiration a constant fraction of gross primary production? *Global Change*
838 *Biology*, 13(6), 1157–1167, doi:10.1111/j.1365-2486.2007.01365.x, 2007.
- 839 Dieguez-Aranda, U., Burkhardt, H. E. and Amateis, R. L.: Dynamic site model for loblolly pine
840 (*Pinus taeda* L.) plantations in the United States, *Forest Science*, 52(3), 262–272, 2006.
- 841 Dietze, M. C., LeBauer, D. S. and Kooper, R.: On improving the communication between
842 models and data, *Plant Cell Environ*, 36(9), 1575–1585, doi:10.1111/pce.12043, 2013.
- 843 Ewers, B. E., Oren, R., Phillips, N., Stromgren, M. and Linder, S.: Mean canopy stomatal
844 conductance responses to water and nutrient availabilities in *Picea abies* and *Pinus taeda*, *Tree*
845 *Physiology*, 21(12-13), 841–850, 2001.
- 846 Fox, A., Williams, M., Richardson, A. D., Cameron, D., Gove, J. H., Quaife, T., Ricciuto, D.,
847 Reichstein, M., Tomelleri, E., Trudinger, C. M. and Van Wijk, M. T.: The REFLEX project:
848 Comparing different algorithms and implementations for the inversion of a terrestrial ecosystem
849 model against eddy covariance data, *Agr Forest Meteorol*, 149(10), 1597–1615,
850 doi:10.1016/j.agrformet.2009.05.002, 2009.
- 851 Fox, T. R., Jokela, E. J. and Allen, H. L.: The Development of Pine Plantation Silviculture in the
852 Southern United States, *Journal of Forestry*, 105(7), 337–347, 2007.
- 853 Gao, C., Wang, H., Weng, E., Lakshmivarahan, S., Zhang, Y. and Luo, Y.: Assimilation of
854 multiple data sets with the ensemble Kalman filter to improve forecasts of forest carbon
855 dynamics, *Ecological Applications*, 21(5), 1461–1473, doi:10.1890/09-1234.1, 2011.
- 856 Gonzalez-Benecke, C. A. and Martin, T. A.: Water availability and genetic effects on water
857 relations of loblolly pine (*Pinus taeda*) stands, *Tree Physiology*, 30(3), 376–392,
858 doi:10.1093/treephys/tpp118, 2010.
- 859 Gonzalez-Benecke, C. A., Gezan, S. A., Albaugh, T. J., Allen, H. L., Burkhardt, H. E., Fox, T. R.,
860 Jokela, E. J., Maier, C. A., Martin, T. A., Rubilar, R. A. and Samuelson, L. J.: Local and general
861 above-stump biomass functions for loblolly pine and slash pine trees, *Forest Ecol Manag*, 334,



- 862 254–276, doi:10.1016/j.foreco.2014.09.002, 2014.
- 863 Gonzalez-Benecke, C. A., Teskey, R. O., Martin, T. A., Jokela, E. J., Fox, T. R., Kane, M. B.
864 and Noormets, A.: Regional validation and improved parameterization of the 3-PG model for
865 *Pinus taeda* stands, *Forest Ecol Manag*, 361, 237–256, doi:10.1016/j.foreco.2015.11.025, 2016.
- 866 Hobbs, N. T. and Hooten, M. B.: *Bayesian Models: A Statistical Primer for Ecologists*, Princeton
867 University Press, Princeton. 2015.
- 868 Iritz, Z. and Lindroth, A.: Energy partitioning in relation to leaf area development of short-
869 rotation willow coppice, *Agr Forest Meteorol*, 81(1-2), 119–130, doi:10.1016/0168-
870 1923(95)02306-2, 1996.
- 871 Keenan, T. F., Carbone, M. S., Reichstein, M. and Richardson, A. D.: The model–data fusion
872 pitfall: assuming certainty in an uncertain world, *Oecologia*, 167(3), 587–597,
873 doi:10.1007/s00442-011-2106-x, 2011.
- 874 Keenan, T. F., Davidson, E., Moffat, A. M., Munger, W. and Richardson, A. D.: Using model-
875 data fusion to interpret past trends, and quantify uncertainties in future projections, of terrestrial
876 ecosystem carbon cycling, *Global Change Biology*, 18(8), 2555–2569, doi:10.1111/j.1365-
877 2486.2012.02684.x, 2012.
- 878 Landsberg, J. and Waring, R.: A generalised model of forest productivity using simplified
879 concepts of radiation-use efficiency, carbon balance and partitioning, *Forest Ecol Manag*, 95(3),
880 209–228, doi:10.1016/S0378-1127(97)00026-1, 1997.
- 881 Le Quere, C., Moriarty, R., Andrew, R. M., Canadell, J. G., Sitch, S., Korsbakken, J. I.,
882 Friedlingstein, P., Peters, G. P., Andres, R. J., Boden, T. A., Houghton, R. A., House, J. I.,
883 Keeling, R. F., Tans, P., Arneeth, A., Bakker, D. C. E., Barbero, L., Bopp, L., Chang, J.,
884 Chevallier, F., Chini, L. P., Ciais, P., Fader, M., Feely, R. A., Gkritzalis, T., Harris, I., Hauck, J.,
885 Ilyina, T., Jain, A. K., Kato, E., Kitidis, V., Klein Goldewijk, K., Koven, C., Landsch utzer, P.,
886 Lauvset, S. K., Lef evre, N., Lenton, A., Lima, I. D., Metzl, N., Millero, F., Munro, D. R.,
887 Murata, A., Nabel, J. E. M. S., Nakaoka, S., Nojiri, Y., O'Brien, K., Olsen, A., Ono, T., P 'erez,
888 F. F., Pfeil, B., Pierrot, D., Poulter, B., Rehder, G., R odenbeck, C., Saito, S., Schuster, U.,
889 Schwinger, J., S 'ef 'erian, R., Steinhoff, T., Stocker, B. D., Sutton, A. J., TAKAHASHI, T.,
890 Tilbrook, B., van der Laan-Luijkx, I. T., van der Werf, G. R., van Heuven, S., Vandemark, D.,
891 Viovy, N., Wiltshire, A., Zaehle, S. and Zeng, N.: *Global Carbon Budget 2015*, *Earth Syst. Sci.*
892 *Data*, 7(2), 349–396, doi:10.5194/essd-7-349-2015, 2015.
- 893 Lu, X., Lu, X., Kicklighter, D. W., Kicklighter, D., Melillo, J. M., Melillo, J. M., Reilly, J. M.,
894 Reilly, J. M., Xu, L. and Wu, L.: Land carbon sequestration within the conterminous United
895 States: Regional- and state-level analyses, *J Geophys Res-Bioge*, 120(2), 379–398,
896 doi:10.1002/2014JG002818, 2015.
- 897 Luo, Y. Q., Luo, Y., Ogle, K., Ogle, K., Tucker, C., Tucker, C., Fei, S., Fei, S., Gao, C., Gao, C.,
898 LaDeau, S., LaDeau, S., Clark, J. S., Clark, J. S. and Schimel, D. S.: Ecological forecasting and
899 data assimilation in a data-rich era, *Ecological Applications*, 21(5), 1429–1442, 2011a.



- 900 Luo, Y., Ogle, K., Tucker, C., Fei, S., Gao, C., LaDeau, S., Clark, J. S. and Schimel, D. S.:
901 Ecological forecasting and data assimilation in a data-rich era, *Ecological Applications*, 21(5),
902 1429–1442, doi:10.1890/09-1275.1, 2011b.
- 903 Luo, Y., Weng, E., Wu, X., Gao, C., Zhou, X. and Zhang, L.: Parameter identifiability,
904 constraint, and equifinality in data assimilation with ecosystem models, *Ecological Applications*,
905 19(3), 571–574, doi:10.1890/08-0561.1, 2009.
- 906 McCarthy, H. R., Oren, R., Johnsen, K. H., Gallet-Budynek, A., Pritchard, S. G., Cook, C. W.,
907 LaDeau, S. L., Jackson, R. B. and Finzi, A. C.: Re-assessment of plant carbon dynamics at the
908 Duke free-air CO₂ enrichment site: interactions of atmospheric [CO₂] with nitrogen and water
909 availability over stand development, *New Phytol*, 185(2), 514–528, doi:10.1111/j.1469-
910 8137.2009.03078.x, 2010.
- 911 McKeand, S., Mullin, T., Byram, T. and White, T.: Deployment of genetically improved loblolly
912 and slash pines in the south, *Journal of Forestry*, 101(3), 32–37, 2003.
- 913 Medlyn, B. E., Zaehle, S., De Kauwe, M. G., Walker, A. P., Dietze, M. C., Hanson, P. J.,
914 Hickler, T., Jain, A. K., Luo, Y., Parton, W., Prentice, I. C., Thornton, P. E., Wang, S., Wang,
915 Y.-P., Weng, E., Iversen, C. M., McCarthy, H. R., Warren, J. M., Oren, R. and Norby, R. J.:
916 Using ecosystem experiments to improve vegetation models, *Nature Climate Change*, 5(6), 528–
917 534, doi:10.1038/nclimate2621, 2015.
- 918 Niu, S., Luo, Y., Dietze, M. C., Keenan, T. F., Shi, Z., Li, J. and III, F. S. C.: The role of data
919 assimilation in predictive ecology, *Ecosphere*, 5(5), art65–16, doi:10.1890/ES13-00273.1, 2014.
- 920 Noormets, A., Gavazzi, M. J., McNulty, S. G., Domec, J.-C., Sun, G., King, J. S. and Chen, J.:
921 Response of carbon fluxes to drought in a coastal plain loblolly pine forest, *Glob Change Biol*,
922 16(1), 272–287, doi:10.1111/j.1365-2486.2009.01928.x, 2010.
- 923 Novick, K. A., Oishi, A. C., Ward, E. J., Siqueira, M. B. S., Juang, J.-Y. and Stoy, P. C.: On the
924 difference in the net ecosystem exchange of CO₂ between deciduous and evergreen forests in the
925 southeastern United States, *Glob Change Biol*, 21(2), 827–842, doi:10.1111/gcb.12723, 2015.
- 926 Oleson, K., Lawrence, D. M., Bonan, G. B., Drewniak, B., Huang, M., Koven, C. D., Levis, S.,
927 Li, F., Riley, W. J., Subin, Z. M., Swenson, S. C., Thornton, P. E., Bozbiyik, A., Fisher, R.,
928 Heald, C. L., Kluzek, E., Lamarque, J. F., Lawrence, P. J., Leung, L. R., Lipscomb, W., Muszala,
929 S., Ricciuto, D. M., Sacks, W., Sun, Y., Tang, J. and Yang, Z. L.: Technical Description of
930 version 4.5 of the Community Land Model (CLM), NCAR Technical Note NCAR, Boulder.
931 2013.
- 932 Oren, R., Ellsworth, D., Johnsen, K., Phillips, N., Ewers, B., Maier, C., Schafer, K., McCarthy,
933 H., Hendrey, G., McNulty, S. G. and Katul, G.: Soil fertility limits carbon sequestration by forest
934 ecosystems in a CO₂-enriched atmosphere, *Nature*, 411(6836), 469–472, doi:10.1038/35078064,
935 2001.
- 936 Pan, Y., Birdsey, R. A., Fang, J., Houghton, R., Kauppi, P. E., Kurz, W. A., Phillips, O. L.,
937 Shvidenko, A., Lewis, S. L., Canadell, J. G., Ciais, P., Jackson, R. B., Pacala, S. W., McGuire,



- 938 A. D., Piao, S. L., Rautiainen, A., Sitch, S. and Hayes, D.: A large and persistent carbon sink in
939 the world's forests, *Science*, 333(6045), 988–993, doi:10.1126/science.1201609, 2011.
- 940 Phillips, N. and Oren, R.: Intra- and inter-annual variation in transpiration of a pine forest,
941 *Ecological Applications*, 11(2), 385–396, 2001.
- 942 Raymond, J. E., Fox, T. R., Strahm, B. D. and Zerpa, J.: Differences in the recovery of four
943 different nitrogen containing fertilizers after two application seasons in pine plantations across
944 the southeastern United States, *Forest Ecol Manag*, 380(C), 161–171,
945 doi:10.1016/j.foreco.2016.08.044, 2016.
- 946 Richardson, A. D., Williams, M., Hollinger, D. Y., Moore, D. J. P., Dail, D. B., Davidson, E. A.,
947 Scott, N. A., Evans, R. S., Hughes, H., Lee, J. T., Rodrigues, C. and Savage, K.: Estimating
948 parameters of a forest ecosystem C model with measurements of stocks and fluxes as joint
949 constraints, *Oecologia*, 164, 25–40, doi:10.1007/s00442-010-1628-y, 2010.
- 950 Sabatia, C. O. and Burkhardt, H. E.: Predicting site index of plantation loblolly pine from
951 biophysical variables, *Forest Ecol Manag*, 326, 142–156, doi:10.1016/j.foreco.2014.04.019,
952 2014.
- 953 Samuelson, L. J., Butnor, J., Maier, C., Stokes, T. A., Johnsen, K. and Kane, M.: Growth and
954 physiology of loblolly pine in response to long-term resource management: defining growth
955 potential in the southern United States, *Can. J. For. Res.*, 38(4), 721–732, doi:10.1139/X07-191,
956 2008.
- 957 Samuelson, L. J., Pell, C. J., Stokes, T. A., Bartkowiak, S. M., Akers, M. K., Kane, M.,
958 Markewitz, D., McGuire, M. A. and Teskey, R. O.: Two-year throughfall and fertilization effects
959 on leaf physiology and growth of loblolly pine in the Georgia Piedmont, *Forest Ecol Manag*,
960 330, 29–37, doi:10.1016/j.foreco.2014.06.030, 2014.
- 961 Shvidenko, A., Barber, C. V. and Persson, R.: Forest and Woodland Systems, in *Ecosystems and
962 Human Well-being Current State and Trends*, Volume, edited by R. Hassan, R. Scholes, and N.
963 Ash, pp. 585–621, Island Press, Washington. 2005.
- 964 Staff, S. S.: Soil Survey Geographic (SSURGO) Database for Southeastern U.S., 2016.
- 965 Subedi, S., Fox, T. and Wynne, R.: Determination of fertility rating (FR) in the 3-PG model for
966 loblolly pine plantations in the Southeastern United States based on site index, *Forests*, 6(9),
967 3002–3027, doi:10.3390/f6093002, 2015.
- 968 Tang, Z., Sayer, M. A. S., Chambers, J. L. and Barnett, J. P.: Interactive effects of fertilization
969 and throughfall exclusion on the physiological responses and whole-tree carbon uptake of mature
970 loblolly pine, *Canadian Journal of Botany*, 82(6), 850–861, doi:10.1139/b04-064, 2004.
- 971 Taylor, K. E., Stouffer, R. J. and Meehl, G. A.: An overview of CMIP5 and the experiment
972 design, *Bull. Amer. Meteor. Soc.*, 93(4), 485–498, doi:10.1175/BAMS-D-11-00094.1, 2012.
- 973 Trudinger, C. M., Raupach, M. R., Rayner, P. J., Kattge, J., Liu, Q., Pak, B., Reichstein, M.,



- 974 Renzullo, L., Richardson, A. D., Roxburgh, S. H., Styles, J., Wang, Y.-P., Briggs, P., Barrett, D.
975 and Nikolova, S.: OptIC project: An intercomparison of optimization techniques for parameter
976 estimation in terrestrial biogeochemical models, *J. Geophys. Res.*, 112(G2), G02027–17,
977 doi:10.1029/2006JG000367, 2007.
- 978 Ward, E. J., Domec, J.-C., Lavinier, M. A., Fox, T. R., Sun, G., McNulty, S., King, J. and
979 Noormets, A.: Fertilization intensifies drought stress: Water use and stomatal conductance of
980 *Pinus taeda* in a midrotation fertilization and throughfall reduction experiment, *Forest Ecol*
981 *Manag.* 355, 72–82, doi:10.1016/j.foreco.2015.04.009, 2015.
- 982 Weng, E. and Luo, Y.: Relative information contributions of model vs. data to short- and long-
983 term forecasts of forest carbon dynamics, *Ecological Applications*, 21(5), 1490–1505,
984 doi:10.1890/09-1394.1, 2011.
- 985 Wightman, M., Martin, T., González-Benecke, C., Jokela, E., Cropper, W., Jr. and WARD, E.:
986 Loblolly Pine Productivity and Water Relations in Response to Throughfall Reduction and
987 Fertilizer Application on a Poorly Drained Site in Northern Florida, *Forests*, 7(10), 214–19,
988 doi:10.3390/f7100214, 2016.
- 989 Will, R., Fox, T., Akers, M., Domec, J.-C., González-Benecke, C., Jokela, E., Kane, M., Lavinier,
990 M., Lokuta, G., Markewitz, D., McGuire, M., Meek, C., Noormets, A., Samuelson, L., Seiler, J.,
991 Strahm, B., Teskey, R., Vogel, J., WARD, E., West, J., Wilson, D. and Martin, T.: A range-wide
992 experiment to investigate nutrient and soil moisture interactions in loblolly pine plantations,
993 *Forests*, 6(6), 2014–2028, doi:10.3390/f6062014, 2015.
- 994 Williams, M., Schwarz, P., Law, B. E., Irvine, J. and Kurpius, M.: An improved analysis of
995 forest carbon dynamics using data assimilation, *Global Change Biology*, 11(1), 89–105,
996 doi:10.1111/j.1365-2486.2004.00891.x, 2005.
- 997 Wutzler, T. and Carvalhais, N.: Balancing multiple constraints in model-data integration:
998 Weights and the parameter block approach, *J Geophys Res-Bioge*, 119(11), 2112–2129,
999 doi:10.1002/2014JG002650, 2014.
- 1000 Zobitz, J. M., Desai, A. R., Moore, D. J. P. and Chadwick, M. A.: A primer for data assimilation
1001 with ecological models using Markov Chain Monte Carlo (MCMC), *Oecologia*, 167(3), 599–
1002 611, doi:10.1007/s00442-011-2107-9, 2011.
- 1003
- 1004



Table 1. A subset of parameters optimized using data assimilation, prior distributions, and the sensitivity of total biomass at age 25 to the parameter. These are the parameters referred to in the results and discussion, other optimized model parameter can be found in the supplemental material.

Parameter	Parameter description	Units	Sensitivity*	Prior distribution	Prior parameters	Reference for prior
α	Canopy quantum efficiency (pines)	mol C mol PAR ⁻¹	0.84	Uniform	Min = 0.02 Max = 0.1	Vague
y	Ratio NPP/GPP	-	0.84	Uniform	Max = 0.66 Min = 0.30	1
fCalpha700	Proportional increase in canopy quantum efficiency between 350 and 700 ppm CO ₂	-	0.08	Uniform	Min = 1.05 Max = 2.0	Vague
fCpFS700	Proportional decrease in allocation to foliage between 350 and 700 ppm CO ₂	-	0.00 [#]	Uniform	Min = 0.50 Max = 1.00	Vague
SWconst	Moisture ratio deficit when downregulation is 0.5	-	0.06	Uniform	Min = 0.6 Max = 1.8	2, Vague
SWpower	Power of moisture ratio deficit	-	0.06	Uniform	Min = 1 Max = 13	2, Vague
FR1	Fertility rating parameter 1 (mean annual temperature coefficient)	-	0.23	Uniform	Min = 0.0 Max = 1.0	Vague
FR2	Fertility rating parameter 2 (site index age 25 coefficient)	-	0.39	Uniform	Min = 0.0 Max = 1.0	Vague
wSx1000	Maximum stem mass per tree at 1000 trees/ha	kg tree ⁻¹	0.43	Normal	Mean = 235 Sd = 25	3,4
thinPower	Power in self thinning law	-	0.25	Uniform	Min = 1.1 Max = 1.80	3,4
pCRS	Ratio of coarse roots to stem allocation	-	0.08	Uniform	Min = 0.15 Max = 0.35	5

1(DeLucia et al., 2007);²(Landsberg and Waring, 1997); ³(Bryars et al., 2013);⁴(Gonzalez-Benecke et al., 2016); 5(Albaugh et al., 2005)

* Sensitivity is 1 when a 10% increase in the parameter results in a 10% change in total biomass. [#]Sensitivity is 0 when a 10% increase in the parameters does not change total biomass by a value greater than 0.01%.



1010

Table 2. Regional observational data streams used in data assimilation.

Data stream	Measurement frequency	Measurement or estimation technique	Uncertainty	Stream ID for Table 4
Foliage biomass (Pine)	Annual or less	Allometric relationship	Based on propagating the allometric model uncertainty in Gonzalez-Benecke et al. 2014. Varied by observation.	1
Foliage biomass (hardwood)	Annual or less	Allometric relationship	Assumed zero	2
Stem biomass (pine)	Annual or less	Allometric relationship	Based on propagating the allometric model uncertainty in Gonzalez-Benecke et al. 2014. Varied by observation.	3
Stem biomass (hardwood)	Annual or less	Allometric relationship	Assumed zero	4
Coarse root biomass (combined)	Annual or less	Allometric relationship	Standard deviation (SD) = 10% of observation	5
Fine root biomass (combined)	Annual or less	Allometric relationship	SD = 10% of observation	6
Foliage biomass turnover (combined)	Annual	Litterfall traps	SD = 2.5% of observation	7
Fine root biomass turnover (combined)	Annual	Mini-rhizotrons	SD = 10% of observation	8
Pine stem count	Annual or less	Counting individuals	1% (assumed small)	9
Leaf area index (pine)	Monthly to annual	Litter traps or LI 2000	If litter trap method: SD = 2.5% of observation If LI-2000 method: SD = 10% of observation	10
Leaf area index (hardwood)	Monthly to annual	Litter traps or LI 2000	If litter trap method: SD = 2.5% of observation If LI-2000 method: SD = 10% of observation	11
Leaf area index (combined)	Only used if not separated into pine and hardwood	Litter traps or LI 2000	If litter trap method: SD = 2.5% of observation If LI-2000 method: SD = 10% of observation	12
Gross Ecosystem Production	Monthly	Modeled from flux eddy-covariance net ecosystem exchange	SD = 10% of observation	13
Evapotranspiration	Monthly	Eddy-covariance	SD = 10% of observation	14

1011
 1012



Table 3. Descriptions of the studies used in data assimilation.

Study name	Number of locations	Number of plots per site	Experimental treatments (plots)	Data streams (Table 2)	Measurement Years	Measurement Stand Ages (years)	Reference
FMRC ¹ Thinning Study	163	1	None	1, 3, 9	1981 - 2003	8 - 30	(Burkhardt et al., 1985)
FPC ² Region-wide 18	18	2	Nutrient addition	1, 3, 9	2011-2014	12-21	(Albaugh et al., 2015)
PINEMAP ³	4	16	Nutrient addition, 30% throughfall, Nutrient x throughfall	1, 3, 9	2011-2015	3 - 13	(Will et al., 2015)
Waycross	1	2	Nutrient addition	3, 9, 10	1991-2010	4-23	(Bryars et al., 2013)
SETRES ⁴	1	16	Nutrient addition, irrigation, nutrient x irrigation	1, 3, 5, 6, 9, 10	1991-2006	8 - 23	(Albaugh et al., 2004)
Duke FACE ⁵ and flux	1	12	CO ₂ , nutrient addition, CO ₂ x nutrient addition	2, 3, 4, 5, 6, 7, 8, 9, 10, 11, 13, 14	1996-2004	13-22	(McCarthy et al., 2010; Novick et al., 2015)
NC2 Flux	1	1	None	2, 3, 4, 5, 6, 7, 9, 10, 11, 12, 13, 14	2005-2014	12-22	(Noormets et al., 2010)
Total	187	294			1981 - 2014	4 - 30	

¹Forest Modeling Research Cooperative; ² Forest Productivity Cooperative; ³ Pine Integrated Network: Education, Mitigation, and Adaptation project (PINEMAP); ⁴ Southeast Tree Research and Education Site; ⁵ Free Air Carbon Enrichment



Table 4. Description of the different data assimilation approaches used.

Simulation Name	Treatments included in assimilation	Number of plots
All	1-stage data assimilation. All plots and experiments in the region were used simultaneously.	294
DK+NC2	1 st stage of 2-stage assimilation. All plots at the Duke eddy flux (DK3), Duke Free Air CO ₂ Enrichment Study, and NC2 eddy flux site; includes CO ₂ enrichment and nutrient addition experiments at the Duke site	13
DK+NC2-fert	1 st stage of 2-stage assimilation. Same as DK+NC2 but without nutrient fertilization plots	10
RW	2 nd stage of 2-stage assimilation. Region-wide assimilation of FRMC, FPC, PINEMAP, Waycross, and SETRES sites. Uses the posteriors of the DK+NC2 simulation as priors. Includes nutrient addition and water manipulation experiments. This simulation is repeated four times for four different out-of-sample validation plots.	281
RW-fert	2 nd stage of 2-stage assimilation. Same as RW but without nutrient addition experiments; uses the posteriors of the DK+NC2-fert simulation as priors	222
RW-water	2 nd stage of 2-stage assimilation. Same as RW but without water manipulation experiments	241

1018
 1019



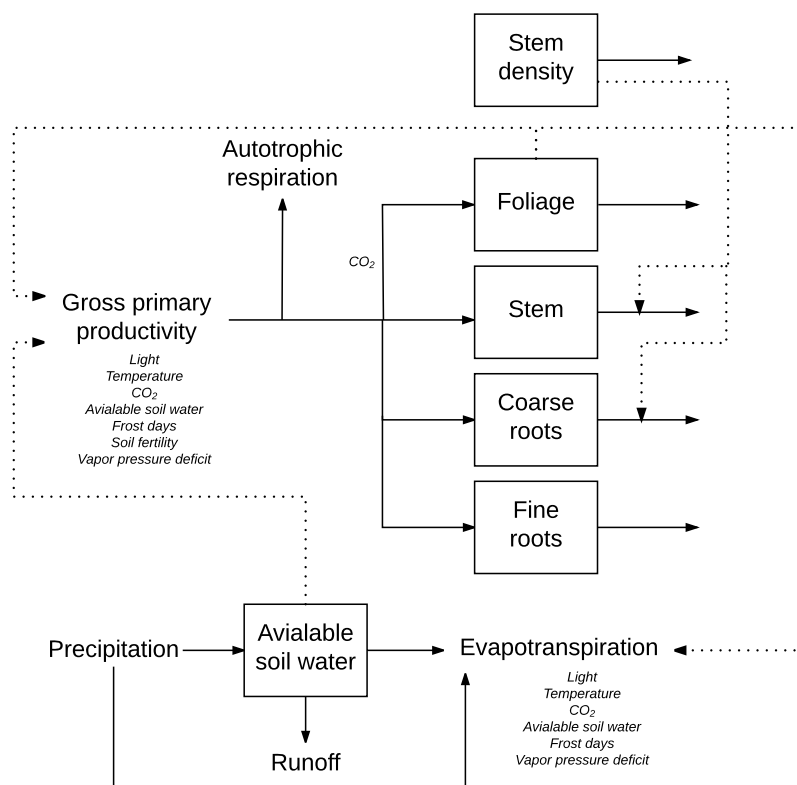
Table 5. Posterior means and 95% credible intervals for parameters listed in Table 1 using the data assimilation approaches listed in Table 4.

Parameter	RW	RW-fert	RW-water	DK+NC2	All
α	0.037 (0.034 – 0.040)	0.040 (0.036 – 0.045)	0.037 (0.035 – 0.040)	0.035 (0.030 – 0.042)	0.032 (0.030 – 0.035)
y	0.48 (0.46 – 0.51)	0.48 (0.45–0.51)	0.48 (0.46 – 0.51)	0.48 (0.45 – 0.51)	0.52 (0.50 – 0.54)
fCalpha700	1.31 (1.22 – 1.40)	1.31 (1.22 – 1.40)	1.31 (1.22 – 1.40)	1.32 (1.23 – 1.41)	1.11 (1.08 – 1.15)
fCpFS700	0.84 (0.75 – 0.93)	0.83 (0.75 – 0.93)	0.84 (0.75 – 0.93)	0.84 (0.76–0.93)	0.99 (0.95 – 1.0)
SWconst	1.48 (1.09 – 1.85)	1.31 (0.95 – 1.70)	1.8 (1.47 – 2.15)	1.30 (0.89 – 1.76)	1.57 (1.08 – 1.79)
SWpower	1.61 (0.90 – 2.46)	1.29 (0.78 – 1.98)	2.93 (1.48 – 3.82)	2.20 (1.47 – 3.44)	1.47 (1.09 – 2.26)
FR1	0.094 (0.086 – 0.104)	0.096 (0.088 – 0.103)	0.118 (0.110 – 0.128)	not fit	0.094 (0.087 – 0.102)
FR2	0.144 (0.133 – 0.154)	0.124 (0.108 – 0.142)	0.179 (0.156 – 0.182)	not fit	0.153 (0.140 – 0.168)
wSx1000	176 (171 – 181)	180 (174 – 186)	180 (176 – 186)	258 (228 – 295)	181 (174 0 187)
thinPower	1.67 (1.60 – 1.74)	1.70 (1.63 – 1.78)	1.71 (1.65 – 1.78)	1.28 (1.12 – 1.60)	1.61 (1.51 – 1.69)
pCRS	0.26 (0.25 – 0.27)	0.24 (0.23 – 0.25)	0.25 (0.24 – 0.26)	0.17 (0.16 – 0.19)	0.28 (0.27 – 0.29)

1020



1021 Figures
 1022



1023 Figure 1. A diagram of the monthly time-step 3-PG model used in this study. The stocks are represented by the
 1024 boxes and the fluxes by the arrows. An influence of a stock on a flux that is not directly related to that stock is
 1025 represented by the dotted lines. The environmental influences on a flux is described using italics. A description of
 1026 the model can be found in the supplemental information.
 1027
 1028
 1029

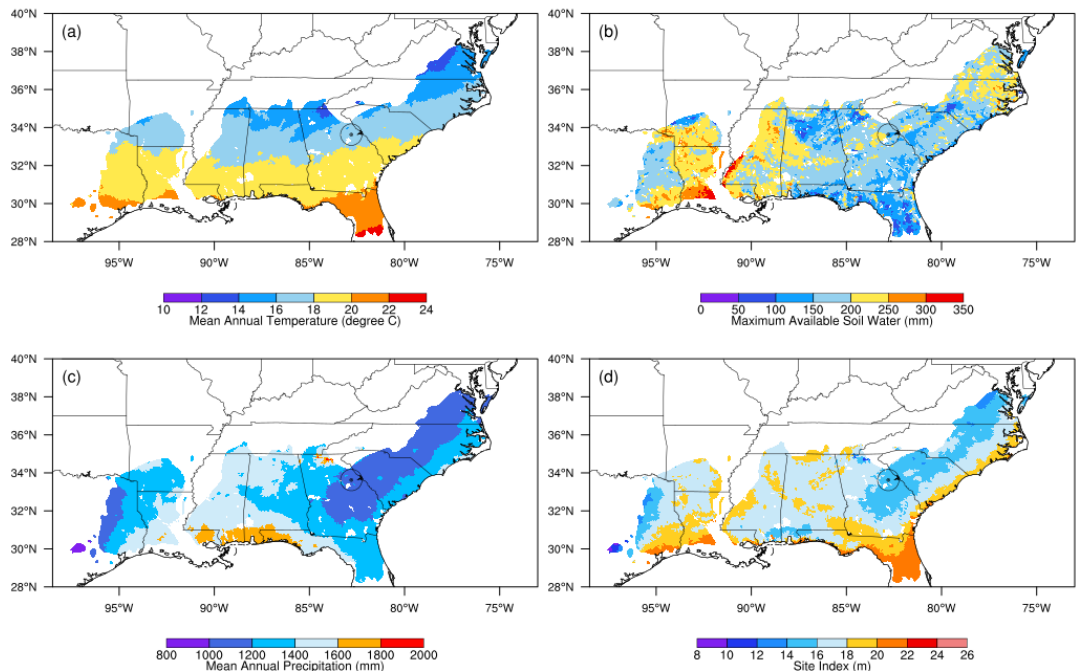


Figure 2. Key climatic and stand characteristic inputs to the regional 3-PG simulations: (a) Mean annual temperature (1979-2011) as a summary of the gradient in monthly temperature inputs used in simulations, (b) maximum available soil water for the top 1.5 meters of soil from SSURGO, (c) mean annual precipitation (1979-2011) as a summary of the gradient in monthly precipitation inputs used in simulations, and (d) site index. The focal site in Georgia highlighted in Figures 5c and 6b is represented by the circle containing the dot. The area shown is the natural range of loblolly pine (*Pinus taeda* L.).

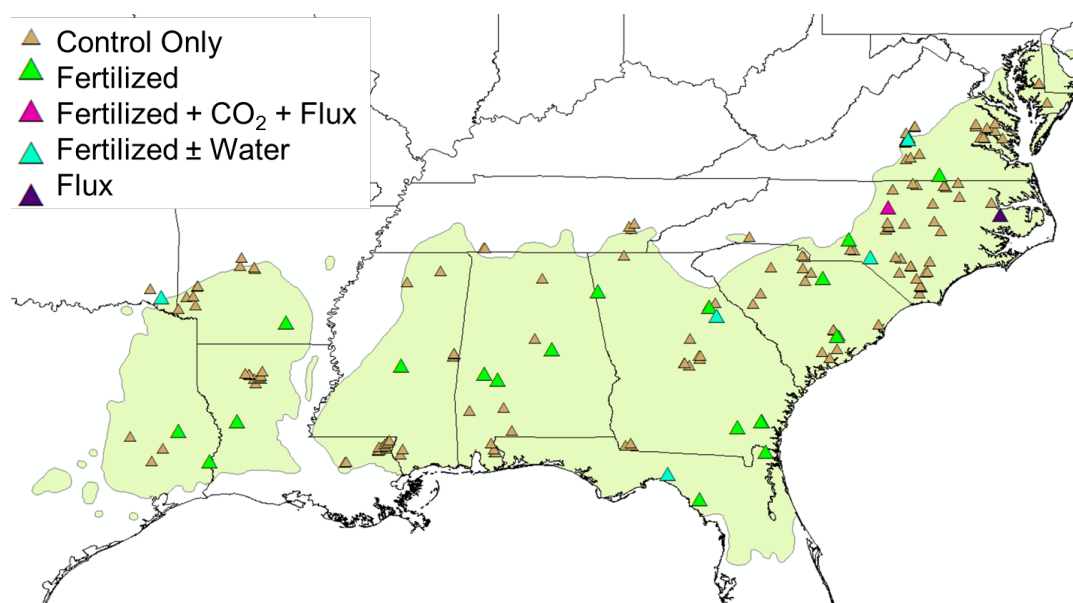
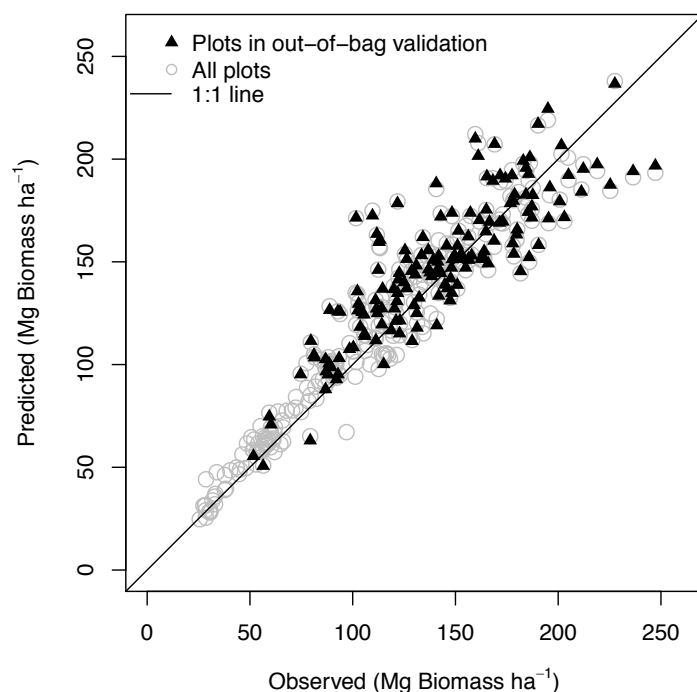


Figure 3. Map of loblolly pine distribution, plot locations used in data assimilation, and the experiment type associated with each plot. The control-only treatments were plots without any associated experimental treatment or flux measurements. Fertilized were plots with nutrient additions. CO₂ were plots with free-air concentration enrichment treatments. The flux treatments were plots with eddy-covariance measurements of ecosystem-scale carbon and water exchange. The water treatments included throughfall exclusion and irrigation experiments.



1050
 1051 Figure 4. Model evaluation of stem biomass using the RW simulation described in Table 5. The
 1052 gray circles correspond to predictions where all plots were used in data assimilation. The black
 1053 triangles correspond to predictions where 120 plots were not included in data assimilation and
 1054 represent an independent evaluation of model predictions (out-of-bag validation). For each plot,
 1055 we used the measurement with the longest interval between initialization and measurement for
 1056 evaluation.

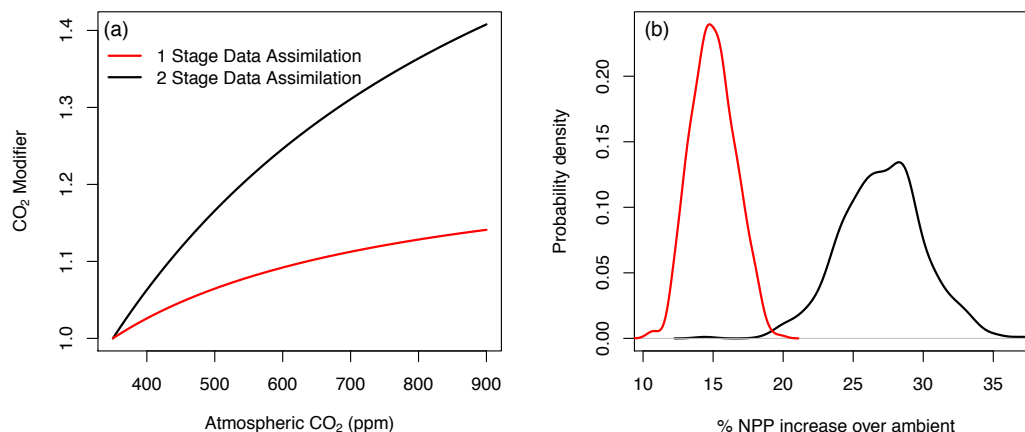


Figure 5. The influence of the data assimilation approach on predictions of how productivity responds to atmospheric CO₂. (a) The relationship between atmospheric CO₂ concentration and the modifier of light-use efficiency when all plots and experiments are assimilated simultaneously (1 stage) and when the Duke and NC2 plots are assimilated before assimilating the remaining observations across the region (2 stage). (b) The probability distribution of predicted response of NPP to the elevated CO₂ at the Duke FACE experiment for the two assimilation approaches. Uncertainty was estimated by integrating the parameter uncertainty estimated through data assimilation (see Methods).

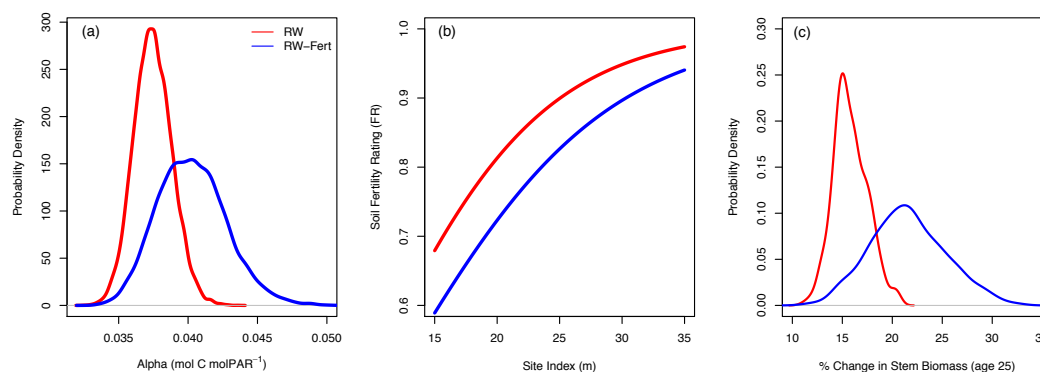
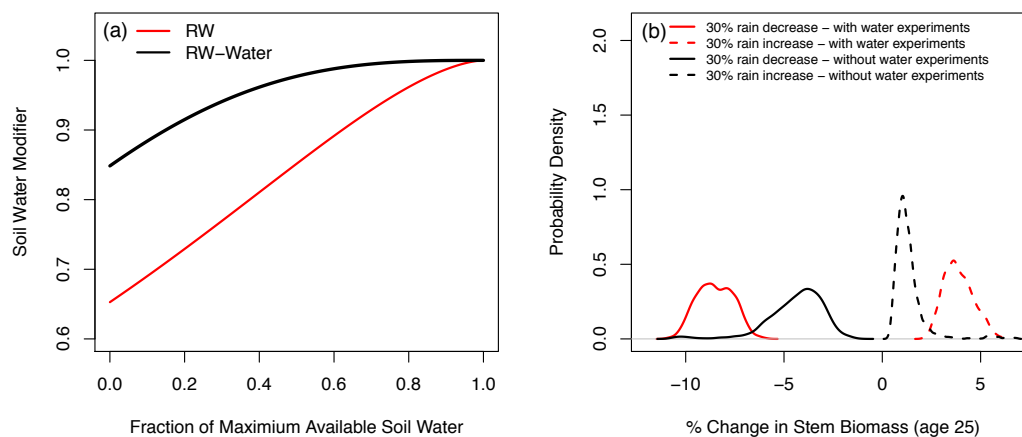


Figure 6. The influence of the data assimilation (DA) approach on predictions of light-use efficiency, nutrient limitation, and how productivity responds to nutrient addition. (a) The posterior distribution for the potential light-use efficiency parameter (alpha). (b) The relationship between site index and the nutrient limitation modifier in 3-PG (FR). (c) The predicted distribution of the response of stem biomass to nutrient fertilization (setting FR = 1) at the focal site in Georgia. The red line corresponds to DA that included nutrient addition experiments. The blue line corresponds to DA that did not include nutrient addition experiments.



1077



1078

1079

1080

1081

1082

1083

1084

1085

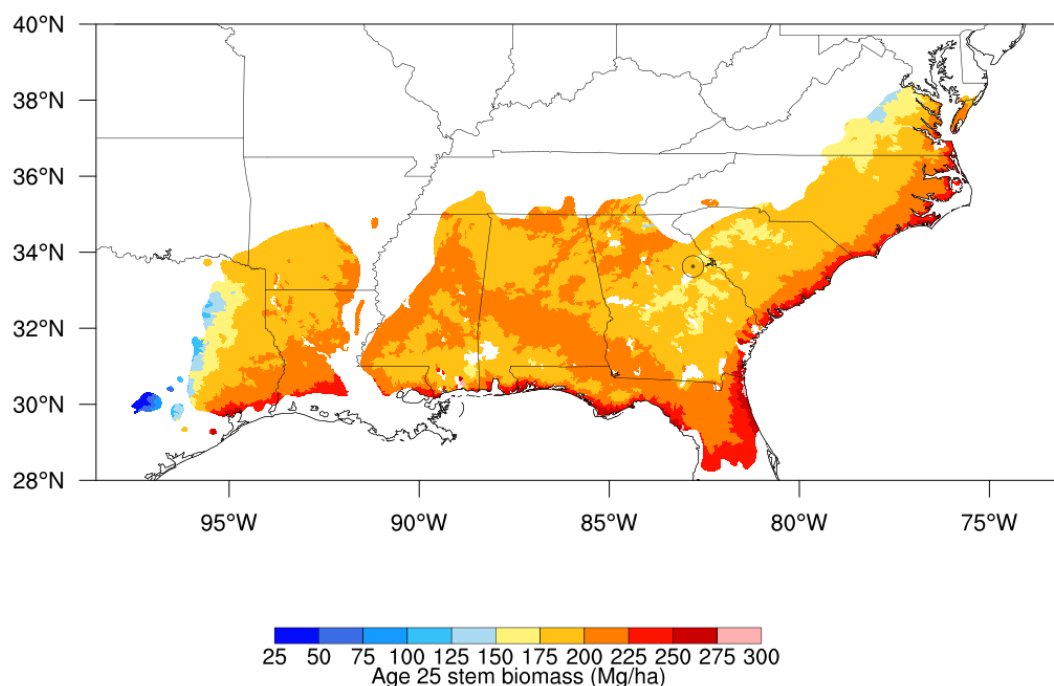
1086

1087

Figure 7. The influence of the data assimilation (DA) approach on predictions of water limitation and how productivity responds to a change in precipitation. (a) The relationship between fraction of maximum available soil water, as predicted by 3-PG, and the modifier of light-use efficiency and canopy conductance. (b) The predicted distribution of the response of stem biomass to a 30% increase (dashed lines) and a 30% decrease (solid lines) in precipitation at the focal site in Georgia. The red line corresponds to DA that included water manipulation experiments. The black line corresponds to DA that did not include water manipulation experiments.



1088



1089

1090

1091

1092

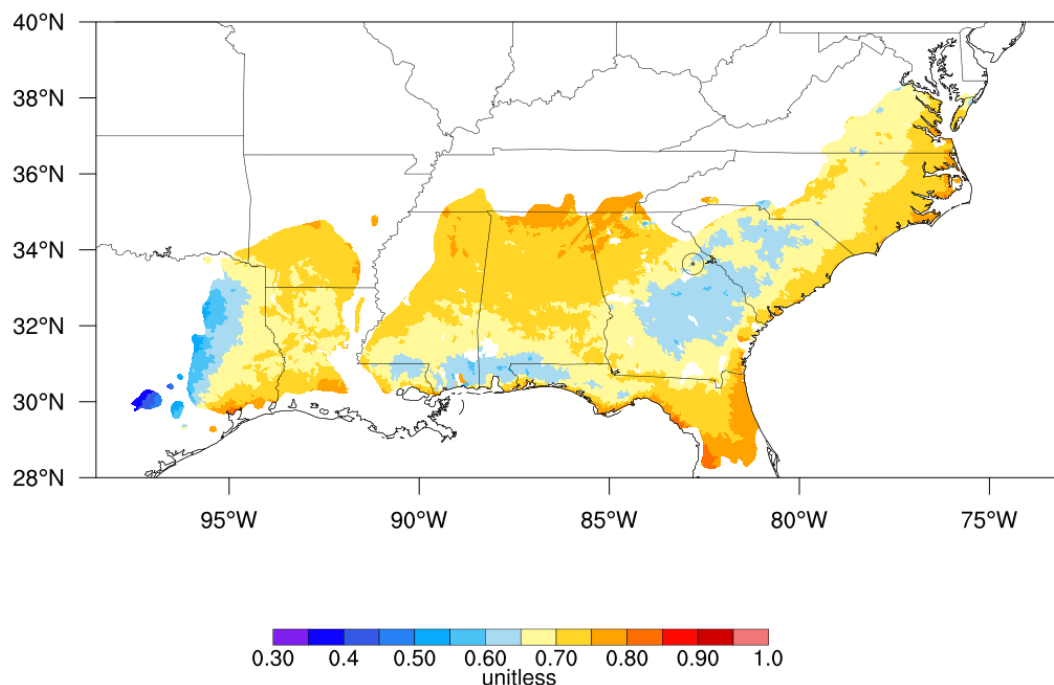
1093

1094

Figure 8. Regional predictions of stem biomass stocks for a 25-year-old stand planted in 1979. Parameters used the predictions were from the RW data assimilation approach described in Table 5. The focal site in Georgia highlighted in Figures 5c and 6b is represented by the circle containing the dot.



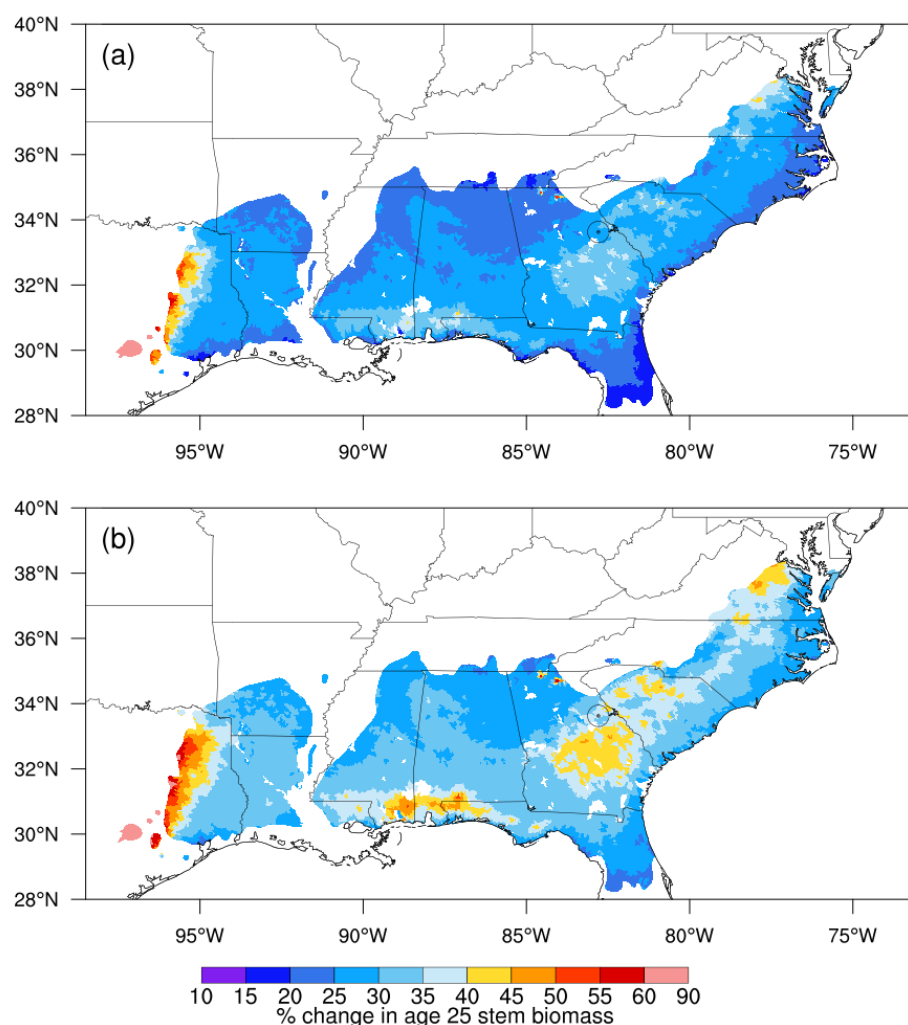
1095
 1096
 1097



1098
 1099 Figure 9: Regional predictions of the soil fertility factor (FR) used in 3-PG to define the nutrient
 1100 status of the simulated stand. Parameters used the predictions were from the RW data
 1101 assimilation approach described in Table 5. The focal site in Georgia highlighted in Figures 5c
 1102 and 6b is represented by the circle containing the dot.



1103



1104

1105

1106

1107

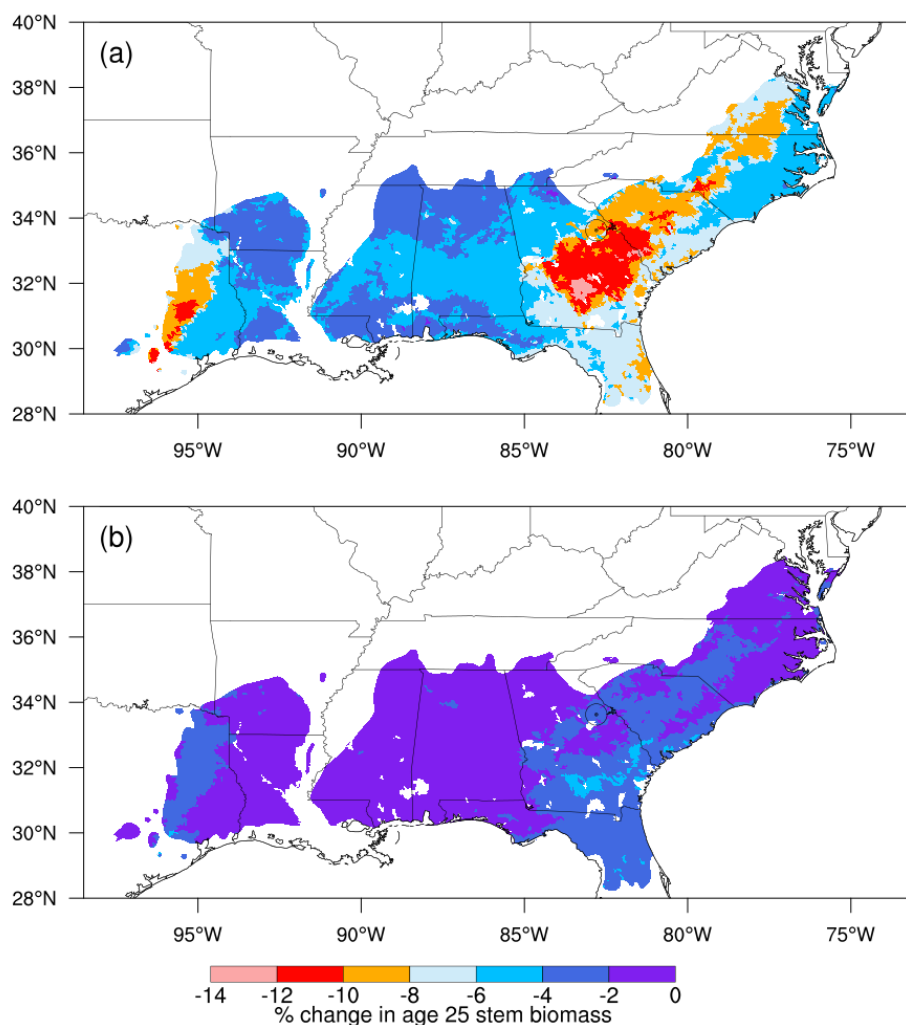
1108

1109

1110

1111

Figure 10: Regional predictions of the change in stem biomass of a 25-year stand when nutrient limitation is completely removed through nutrient addition (simulated by setting $FR = 1$). Predictions from data assimilation that included nutrient addition experiments are shown in (a) and prediction data assimilation that did not include nutrient addition experiments are shown in (b). The focal site in Georgia highlighted in Figures 5c and 6b is represented by the circle containing the dot.



1112
 1113 Figure 11. Regional predictions of the change in stem biomass of a 25-year stand when annual
 1114 precipitation is reduced by 30%. Predictions from data assimilation that included water
 1115 manipulation experiments are shown in (a) and prediction data assimilation that did not include
 1116 water manipulation experiments are shown in (b). The focal site in Georgia highlighted in
 1117 Figures 6c and 7b is represented by the circle containing the dot.
 1118